VOLUME 19, 1957/58, No. 11 pp. 301-332 Published 31st May 1958

Philips Technical Review

DEALING WITH TECHNICAL PROBLEMS
RELATING TO THE PRODUCTS, PROCESSES AND INVESTIGATIONS OF
THE PHILIPS INDUSTRIES

PARAMAGNETIC RESONANCE

by J. S. van WIERINGEN.

538.222

The investigation of the phenomenon of paramagnetic resonance, discovered in 1945, has proved to be a valuable tool in the study of the solid state. For this phenomenon to occur the substance must contain a number of "atomic magnets" (paramagnetic atoms or ions, colour centres, donors or acceptors in semi-conductors, organic radicals). The specimen for examination is placed in a microwave resonant cavity, to which energy is supplied via a waveguide, the whole being placed in a magnetic field of variable strength. The resonance spectrum (reflected power as a function of the applied field) then provides important information on the properties of the crystal lattice.

The phenomenon of paramagnetic resonance

In 1945 Zavoisky discovered the phenomenon, predicted by Gorter and Kronig as early as 1936 [1]), that paramagnetic ions in a crystal subjected to a constant magnetic field (of induction B) are capable of absorbing energy from a superimposed high-frequency alternating magnetic field (of frequency f_r). This occurs when the following relation is fulfilled:

$$f_r = g \frac{e}{4\pi m} B, \quad \ldots\ldots \quad (1)$$

where e is the charge on the electron (1.6×10^{-19} coulomb), m its mass (9×10^{-31} kg), and g a factor approximately equal to 2. Since this absorption occurs in a very narrow frequency range, it is referred to as paramagnetic resonance absorption, or simply as paramagnetic resonance. It was later found that the phenomenon occurs not only with paramagnetic ions, but also with colour centres, with donors and acceptors in semiconductors, and with organic radicals — all being cases in which "atomic magnets" are present in the substance. With an applied field $B \approx 0.3$ Wb/m^2 [3000 gauss], the frequencies f_r are of the order of 10^4 Mc/s.

In a given magnetic field the absorption usually takes place not at one specific frequency given by (1), but rather at a number of frequencies f_1, f_2 etc. in the neighbourhood of f_r. The paramagnetic absorption line is thus split into several components; the resulting pattern, defined by the differences f_1-f_r, f_2-f_r, etc. depends on various factors, in the first place on the nature of the atomic magnets, and further on the crystal lattice in which the atomic magnets are situated. Moreover, the line width of the components also varies, this depending on the crystal lattice, the concentration of the atomic magnets, lattice defects and other factors. A study of the paramagnetic absorption spectra, therefore, enables one to obtain information on the electrical fields in which the ions in the crystal are situated, and on the behaviour of the electron orbits in these fields. The investigation of paramagnetic resonance is thus an additional method for the study of the solid state, and takes its place alongside other methods such as the investigation of electrical conductivity, thermo-electric power, Hall effect, X-ray diffraction and so on.

In view of the increasing interest in the properties of solids it is not surprising that a vast amount of research has been carried out in the field of paramagnetic resonance since 1945. More than 400

[1]) C. J. Gorter and R. de L. Kronig, Physica **3**, 1009, 1936; E. Zavoisky, J. Phys. USSR **9**, 211, 1945 (also ibid. **10**, 170 and 197, 1946).

publications have appeared on the subject [2]).

In this article we shall discuss some aspects of this research, including investigations carried out in the Philips laboratories at Eindhoven. First of all we shall briefly review the theory of paramagnetic resonance.

For the readers' convenience some facts on paramagnetism and ferromagnetism are recapitulated here.

Besides an electric charge an electron possesses a magnetic moment, associated with an angular momentum (spin). Since atoms consist of a nucleus, surrounded by an electron cloud, it may be expected that all atoms will exhibit magnetic properties, not only because of the magnetic moments of the individual electrons but also because the electrons describe orbits around the nucleus, which we may regard as circular currents.

In general, free atoms are found to have a magnetic moment which is the resultant of the spin and orbital moments of the individual electrons. It should be recalled here that most of the electrons move in closed shells and that the resultant of the spin and orbital moments for such a shell is zero. For instance, the atoms of the inert gases have no resultant moment since their electron cloud consists entirely of closed shells. The same applies to the ions of which the crystal lattices of most inorganic solids are built up. There are, however, ions whose electron cloud does not have the "inert-gas structure", one or more of their shells not being completely filled. These ions show a resultant moment which can be oriented in an external magnetic field. Substances containing these ions thus have a positive magnetic susceptibility, i.e. they are paramagnetic. The most familiar paramagnetic ions are those in compounds of the iron group (e.g. V^{3+}, Cr^{3+}, Mn^{2+}, Fe^{2+}, Fe^{3+}, Co^{2+}, Ni^{2+}), in which the outermost electron shell is incompletely occupied, and the rare-earth ions, which owe their paramagnetic properties to the fact that one of the inner shells is not completely filled.

Some metals are also paramagnetic. Generally speaking, metals consist of an ion lattice between which electrons move more or less freely. The orbital motion of most of the electrons is such that their spin and orbital moments compensate each other — analogous to the compensation for the majority of electrons in the electron cloud of a free atom — and only a few electrons are able (particularly at higher temperatures) to contribute to the paramagnetism. As a rule, therefore, the paramagnetism is weak (Na, Ca) [3]).

In this article we are not concerned with the paramagnetism of metals, but rather with that of certain semi-conductors, which is due to the presence of foreign atoms (donors, acceptors) or to the electrons or "electron holes" ceded to the lattice by these atoms; these electrons or holes function as atomic magnets.

Where the interaction between the atomic magnets in a substance is such that they are in spontaneous parallel orientation, the substance is ferromagnetic. In that case, even in the absence of an external magnetic field, a macroscopic magnetic moment is present in the Weiss domains into which the substance is divided. Ferromagnetism, which occurs only in a few metals (Fe, Co, Ni, Gd) and certain compounds thereof, in certain Mn alloys and in ferrites, will be touched on in passing in the following discussion of the theory.

Theory of paramagnetic resonance

In general, paramagnetism is due to the spin and orbital moments of the electrons. For reasons which will later be discussed, the orbital moment can usually be neglected to a first approximation in solids.

According to quantum mechanics, the angular momentum of one ion (in our case the resultant of the electron spins of that ion) can only assume discrete values. Quite generally, the angular momentum may be represented by $\sqrt{S(S+1)}\,(h/2\pi)$, where S is a multiple of $\frac{1}{2}$.

Let us first consider a free electron, in which case $S = \frac{1}{2}$. In a magnetic field B an electron can take up only two kinds of positions, the component of the angular momentum in the direction of B being either $\frac{1}{2}(h/2\pi)$ or $-\frac{1}{2}(h/2\pi)$. The component of the magnetic moment is proportional to this angular momentum, the constant of proportionality being $g_e(e/2m)$, where $g_e = 2.0023$. The two positions S correspond to two energy levels:

$$E = \pm g_e \frac{e}{2m} \times \tfrac{1}{2} \frac{h}{2\pi} B. \quad . \ . \ . \quad (2)$$

Hence the difference in energy between the two levels is

$$\Delta E = g_e \frac{eh}{4\pi m} B. \quad . \ . \ . \ . \ . \quad (3)$$

Similar reasoning applies to an arbitrary paramagnetic ion. This can take up a number of positions with respect to the field B, such that the component of the angular momentum in the direction of the field is equal to $m_s(h/2\pi)$. The number m_s can assume values between $+S$ and $-S$, such that the difference between successive values is equal to 1. For example, where $S = \frac{5}{2}$, m_s may be equal to $\frac{5}{2}$, $\frac{3}{2}$, $\frac{1}{2}$, $-\frac{1}{2}$, $-\frac{3}{2}$ or $-\frac{5}{2}$, totalling $2S+1 = 6$ values. The energy difference between successive levels is again given by (3). *Fig. 1* shows schematically the possible orientations of the angular momentum with respect to the field, and the associated energy levels for a number of values of S, i.e. for a number of different ions. (Different values of S can also be found for one and the same ion, depending on the electron distribution; in general, an atom in an excited state

[2]) We cite here only a number of survey articles covering the subject:
B. Bleaney and K. W. H. Stevens, Paramagnetic resonance, I, Rep. Progr. Phys. **16**, 108-159, 1953.
K. D. Bowers and J. Owen, Paramagnetic resonance, II, Rep. Progr. Phys. **18**, 304-373, 1955.
J. E. Wertz, Nuclear and electronic spin magnetic resonance, Chem. Rev. **55**, 829-955, 1955.
D. J. E. Ingram, Spectroscopy at radio and microwave frequencies, Butterworth, London 1955.

[3]) In some metals (e.g. Cu) the weak paramagnetism is dominated by the diamagnetism present in all substances; this is due to the circumstance that an external magnetic field gives rise to a weak and oppositely oriented magnetic moment in the electron cloud of the atom (negative susceptibility).

may have a value of S different from that obtaining for the ground state.)

According to quantum theory, the emission of electromagnetic radiation takes place during the transition from one state with energy E_2 to as tate with energy E_1 ($E_2 > E_1$), and absorption takes place with the reverse transition. The frequency f of the emitted or absorbed radiation is determined by the relation [4])

$$hf = E_2 - E_1. \quad . \quad . \quad . \quad . \quad . \quad (4)$$

Now a quantum-mechanical treatment shows that, in each case, transitions are possible only between successive energy levels. The frequencies are therefore always given by $hf = \Delta E$, where ΔE is given by (3).

Transitions between the levels can occur when an alternating magnetic field is applied at right angles to the field B, the frequency f_r of the alternating field being given by $hf_r = \Delta E$, i.e.,

$$hf_r = g_e \frac{eh}{4\pi m} B. \quad . \quad . \quad . \quad . \quad . \quad (5)$$

During these transitions, energy in the form of quanta hf_r is absorbed from the alternating field or given up to it. This energy-absorption phenomenon is essentially the paramagnetic resonance absorption. In fact, the condition (5) is identical with (1) if we substitute for g the accurate value g_e (= 2.0023).

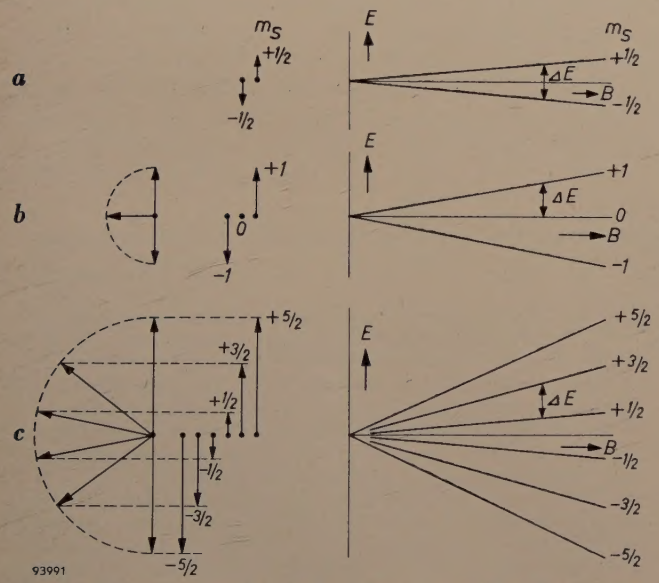

Fig. 1. Quantum-mechanical explanation of the phenomenon of resonance. A dipole having an angular momentum (quantum number S) and an associated magnetic moment can orient itself in only $2S+1$ different ways with respect to an external magnetic field B. The component of the angular momentum parallel to B, $m_s(h/2\pi)$, can assume any of $2S+1$ discrete values, where $S > m_s > -S$. This gives rise to $2S+1$ energy levels, and transitions are possible only between successive levels, of energy difference ΔE. The resonance frequency is given by $hf_r = \Delta E$. The possible orientations of the dipole and the associated energy levels as a function of B are drawn for *a*) $S = \frac{1}{2}$ (case of a single electron), *b*) $S = 1$, *c*) $S = \frac{5}{2}$ (case of the Mn^{2+} ion).

In order to be able to observe resonance absorption an additional effect must appear, for, at resonance, the paramagnetic ions are also continually yielding energy quanta hf_r to the field (so-called stimulated emission [5])). Absorption can only be observed when the number of absorbed quanta exceeds that of the emitted quanta so that, on the average, energy is absorbed from the field. This can indeed occur by interaction between the atomic magnets and their environment.

Let us first consider N entirely free electrons, so that we have two energy levels, differing by ΔE as given by (3), the lower level being occupied by n_1 and the upper by n_2 electrons ($n_1 + n_2 = N$). A high-frequency magnetic field with frequency f_r causes energy transitions in both directions with equal probability. If the lower level was initially more densely occupied ($n_1 > n_2$), then n_1 will decrease and n_2 increase, until $n_1 = n_2 = \frac{1}{2}N$. The number of absorption processes, which is determined by n_1, is then equal to the number of emission processes, which is determined by n_2, and the net result is that no energy is absorbed from the field.

In the case of ions forming part of a crystal lattice, interaction will occur between the electrons and the lattice, as a result of which a state of thermal equilibrium will tend to be set up. For the sake of simplicity we assume that we are concerned with ions, the paramagnetism of which is due to only one electron ($S = \frac{1}{2}$). Hence there are again two energy states. In thermal equilibrium,

$$n_2/n_1 = \exp(-\Delta E/kT), \quad . \quad . \quad . \quad . \quad (6)$$

where k is Boltzmann's constant ($k = 1.38 \times 10^{-23}$ J/°K).

In this case, according to (6), $n_1 \gg n_2$ in the state of equilibrium. The number of absorptions therefore exceeds that of the emissions, so that now the net result is that energy is absorbed from the field. Although the predominating absorption tends to increase the occupation n_2 of the higher level, the absorption nevertheless continues, since, owing to the interaction with the crystal lattice, a portion of the absorbed energy is given up to the lattice as heat. This process (paramagnetic relaxation) is usu-

[4]) This is the familiar Bohr formula. In atomic theory the symbol ν is usually used for the frequency. Since in the present case the frequencies lie in the region of radio waves, the symbol f common in electrical engineering is used here.

[5]) Besides stimulated emission there is, in general, emission due to spontaneous transitions. This is important in optical spectra, but in our case it may be neglected, the frequencies and hence the probabilities being much lower.

ally so fast that, at the high-frequency energies commonly used, the ratio n_2/n_1 differs only very slightly from the equilibrium ratio (6), in spite of the presence of the alternating magnetic field [6]).

According to equation (5) it should be possible to observe the effect of paramagnetic resonance absorption even at relatively low frequencies and correspondingly low magnetic inductions. A limit is set to this, however, by the fact (which does not arise in the simple theory given here) that all transition probabilities diminish with decreasing frequency, so that the whole effect finally becomes too small to be detected. This is the reason that paramagnetic resonance was not discovered until sufficient advances had been made in the development of microwave techniques (frequencies of the order of 1000 Mc/s). Moreover, it is only at such very high frequencies that the apparatus has sufficient resolving power for observing the finer details of the resonance phenomenon, which will be discussed below and on which the practical application of paramagnetic resonance is based.

Relation between paramagnetic resonance and other phenomena

Zeeman effect

In 1896 the Dutch physicist Zeeman discovered that the spectral lines of substances split up into two or more components when the atoms are subjected to a magnetic field. The amount Δf of the splitting (difference between the frequency of a component and the frequency of the unsplit line) is given by the formula:

$$\Delta f = a \frac{e}{4\pi m} B, \quad \ldots\ldots\ldots (7)$$

in which a is a numerical factor equal to a small integer or to a simple fraction. This phenomenon of "magnetic splitting" (Zeeman effect) was also found to occur in those crystals exhibiting sharp absorption lines.

The similarity of equations (7) and (1) points to a close relationship between the two phenomena. The nature of this relationship is discussed below.

We have seen how an energy level of the atom (or ion) in question is split up in a magnetic field into several sub-levels. This process occurs at each of the energy levels corresponding to different electron distributions (orbits) in the atom; see *fig. 2a*. With the Zeeman effect, as well as with paramagnetic resonance, transitions are observed between these sub-levels. In the case of paramagnetic resonance, however, the transition takes place between two sub-levels which have originated from *one* energy level, usually the lowest, of the atom; during the transition only the orientation of the magnetic moment changes (R in fig. 2*a*). With the Zeeman effect, on the other hand, the transitions take place between the sub-levels which have originated from *different* energy levels (e.g. from the ground state and an excited state — σ, π in fig. 2*a*); during the transition there is a change not only in the orientation of the magnetic moment but also in the electron distribution in the atom.

It can be seen that the energy difference — and hence the frequency — is much greater for the Zeeman transitions than for the paramagnetic resonance phenomenon. In the first case the frequencies come within the optical range, which is why the Zeeman effect was discovered so much earlier than paramagnetic resonance. Owing to the greater probabilities of transitions in the optical range, the Zeeman effect is a "strong" effect in that it can be observed in rarefied gases. For paramagnetic resonance to be observable, higher concentrations of atomic magnets are necessary, as in solids, for example. In that case the Zeeman effect is often difficult to observe because of the considerable broadening of the energy levels, particularly those of excited states.

In special cases paramagnetic resonance has been used to produce transitions between sub-levels originating from a higher (excited) level [7]). A particular case in point is mercury vapour. The changed occupation of the sub-levels in the excited state becomes manifest in this case in a change of the relative intensity of the Zeeman components (see fig. 2*b*). This is indeed a very elegant confirmation of the relation between the two phenomena.

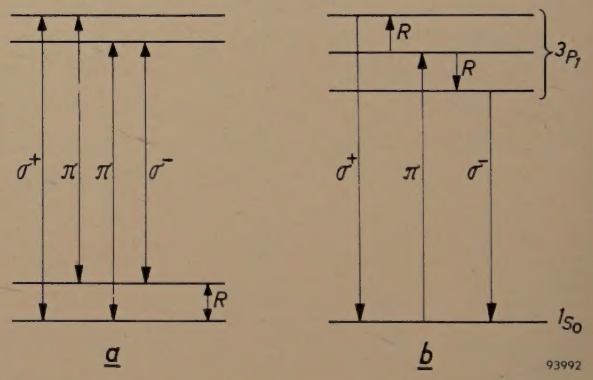

Fig. 2. *a*) Energy levels of a paramagnetic atom in a magnetic field. The ground level and one excited level are shown, both of which are split into two sub-levels by the magnetic field. The long arrows represent transitions for the Zeeman effect, and the short arrow R represents the transition between the sub-levels of the ground state, corresponding to paramagnetic resonance. The components π vibrate in the direction of the field, the components σ perpendicular thereto.
b) Experiments by Brossel and Bitter on the modification of the Zeeman pattern caused by transitions occurring between the sub-levels of an excited level in mercury vapour. Polarized radiation of 2537 Å excites mercury atoms via the π transition into the intermediate of the three $^3P_1$ levels. They drop back via the π transition. However, if the transitions R between the $^3P_1$ sub-levels are made to occur simultaneously, the two σ transitions also occur. These can be detected by the fact that their polarization differs from that of the π transition.

Ferromagnetic resonance

The phenomenon of paramagnetic resonance is also closely related to the phenomenon of ferromagnetic resonance, predicted in 1935 by Landau and Lifshitz and subsequently found with various ferromagnetic substances. Several articles on

[6]) This is opposed to the case of "nuclear spin resonance", where there are appreciable shifts in the equilibrium ratio. See H. G. Beljers, Measurement of magnetic fields by the proton resonance method, Philips tech. Rev. **15**, 55-62, 1953/54.

[7]) J. Brossel and F. Bitter, A new "double resonance" method for investigating atomic energy levels. Application to Hg $^3P_1$, Phys. Rev. **86**, 308-316, 1952.

ferromagnetic resonance (also referred to as gyromagnetic resonance) have appeared in this Review [8]).

Since this phenomenon is concerned with the magnetic moment of all the electrons in a macroscopic domain (Weiss domain), it can be explained in terms of classical as well as quantum theory. The total angular momentum, with the resultant magnetic moment parallel to it, then behaves like a spinning top whose axis, under the influence of a constant external magnetic field, describes a cone with a precession frequency

$$f_p = g_e \frac{e}{4\pi m} B. \quad \ldots\ldots\ldots \quad (8)$$

It is clear that by means of a field rotating in unison with the precession, or by an alternating field at right angles to B, it is possible to influence this motion, and that mechanical resonance (now in the literal meaning of the term) will occur if the frequency f_r of the alternating field is equal to f_p; we then have equation (1) once more.

With a certain reservation, this classical treatment can also be applied to the atomic magnets discussed above, which makes the term paramagnetic "resonance" rather more acceptable. We have preferred to give the quantum-mechanical description, however, since it is indispensable for studying the details of paramagnetic resonance to be discussed below.

Although both phenomena are thus essentially identical, ferromagnetic resonance absorption is much stronger than the paramagnetic effect. Moreover, there is an important qualitative difference as regards the influence of the immediate environment of the atomic magnets. If this environment differs for individual magnets (e.g. in respect to the magnetic moment of neighbouring atomic nuclei) this will manifest itself, as we shall see, in a splitting or broadening of the paramagnetic resonance line. With ferromagnetic resonance, however, individual differences of environment are not noticeable since the atomic magnetic moments are all tightly coupled, and therefore these differences are averaged out.

Apparatus for measurements of paramagnetic resonance

A diagram of the set-up used for our investigations of paramagnetic resonance is given in *fig. 3*. As explained in the foregoing, paramagnetic resonance may be expected when atomic magnets in an external magnetic field are subjected to a transverse high-frequency field. This is done in the present apparatus by introducing the specimen into a resonant cavity T, which is subjected to a variable magnetic field B [9]). The resonant cavity is tuned to the frequency of a microwave generator (klystron K); the output from the klystron is transmitted to the resonant cavity via a waveguide G. The resonant cavity is tuned and matched to the waveguide in the absence of the external magnetic field. The klystron output is then used to keep the resonant cavity in oscillation, and only a weak signal is reflected into the waveguide. This being done, the magnetic field is increased until paramagnetic resonance sets in. This becomes manifest in a change in the tuning and matching of the resonant cavity. As a result the reflected signal increases. By means of a directional coupler R_2 the reflected signal is first separated from the much stronger wave travelling directly from the klystron. It is then detected, in our case by a sensitive superheterodyne method.

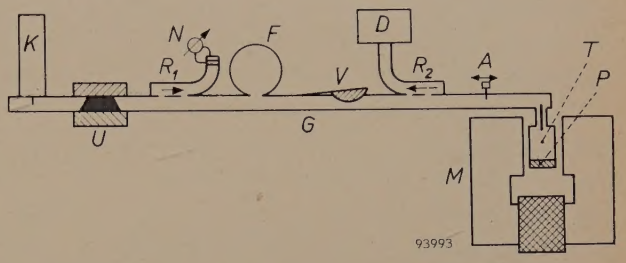

Fig. 3. Experimental set-up for observing paramagnetic resonance. K, klystron, which generates a wave of constant frequency f in the waveguide G. T, resonant cavity placed in the field of electromagnet M. P, specimen in resonant cavity. R_2, directional coupler, which conducts to detector D the signal reflected from T via matching stub A. The amplified detector output is automatically recorded as a function of the external field B. U, ferrite isolator, which prevents the reflected wave from affecting the klystron. The signal fed to T is controlled by a wavemeter F and a level-meter N with directional coupler R_1. V is a variable attenuator.

The reflection coefficient γ of a resonant cavity at the end of a waveguide depends on the damping and detuning and on the strength of the coupling between resonant cavity and waveguide, according to the formula:

$$\gamma = \frac{(1/Q_1) - (1/Q_2) - 2j(\Delta\omega/\omega_0)}{(1/Q_1) + (1/Q_2) - 2j(\Delta\omega/\omega_0)}. \quad \ldots\ldots \quad (9)$$

Here Q_1 is the "external" figure of merit of the resonant cavity (being the value of Q when only the losses through the coupling hole are taken into account); Q_2 is the figure of merit of the resonant cavity without coupling hole; $\omega_0 = 2\pi f_0$, where f_0 is the resonance frequency of the resonant cavity without external field; $\Delta\omega = 2\pi(f - f_0)$, in which f is the imposed frequency.

A paramagnetic specimen P placed in the resonant cavity and subjected to a suitable magnetic field will exhibit paramagnetic resonance (absorption and associated dispersion). This causes a change in the damping (Q_2) and in the tuning ω_0 of the resonant cavity, and hence also in $\Delta\omega$. In most cases only the paramagnetic resonance absorption is of interest, i.e. the increase in damping. According to formula (9), however, the reflected wave is in general dependent both on the change in the tuning (i.e. in $\Delta\omega$) and on the change in the damping (Q_2). The reflected waves, due to the increased damping or to detuning, differ in phase. By suitably choosing the operating point (Q_1, $\Delta\omega$) or by introducing an extra wave with the aid of the matching stub A (fig. 3), one can arrange for the detector to receive a wave which depends only on the damping.

---

[8]) H. G. Beljers and J. L. Snoek, Gyromagnetic phenomena occurring with ferrites, Philips tech. Rev. **11**, 313-322, 1949/50. H. G. Beljers, Amplitude modulation of centimetre waves by means of ferroxcube, Philips tech. Rev. **18**, 82-86, 1956/57 (No. 3). H. G. Beljers, The application of ferroxcube in unidirectional waveguides and its bearing on the principle of reciprocity, Philips tech. Rev. **18**, 158-166, 1956/57 (No. 6).

[9]) See also the article by H. G. Beljers and J. L. Snoek quoted under [8]).

The observations are carried out by leaving the frequency of the klystron constant and by examining the indication of the detector as a function of the magnetic field B, which is slowly varied about a specific value. This function, the "B spectrum", is made visible on an oscilloscope by modulating B at low frequency (equal to the frequency of the oscilloscope time base) and by making the vertical deflection on the oscilloscope proportional to the signal from the detector. *Fig. 4* shows a photograph of the complete apparatus.

In special cases much lower frequencies have been used, for example $f = 10^6$ c/s ($\lambda = 300$ m). This is possible if the spectra concerned are narrow (small Δf with constant B), that is to say if a single, narrow resonance line is to be examined, as in the case of organic radicals.

The normal method of calibrating the field is to record a comparison spectrum for a substance of known paramagnetic properties.

In view of the present wide application of paramagnetic resonance, Philips are now marketing a

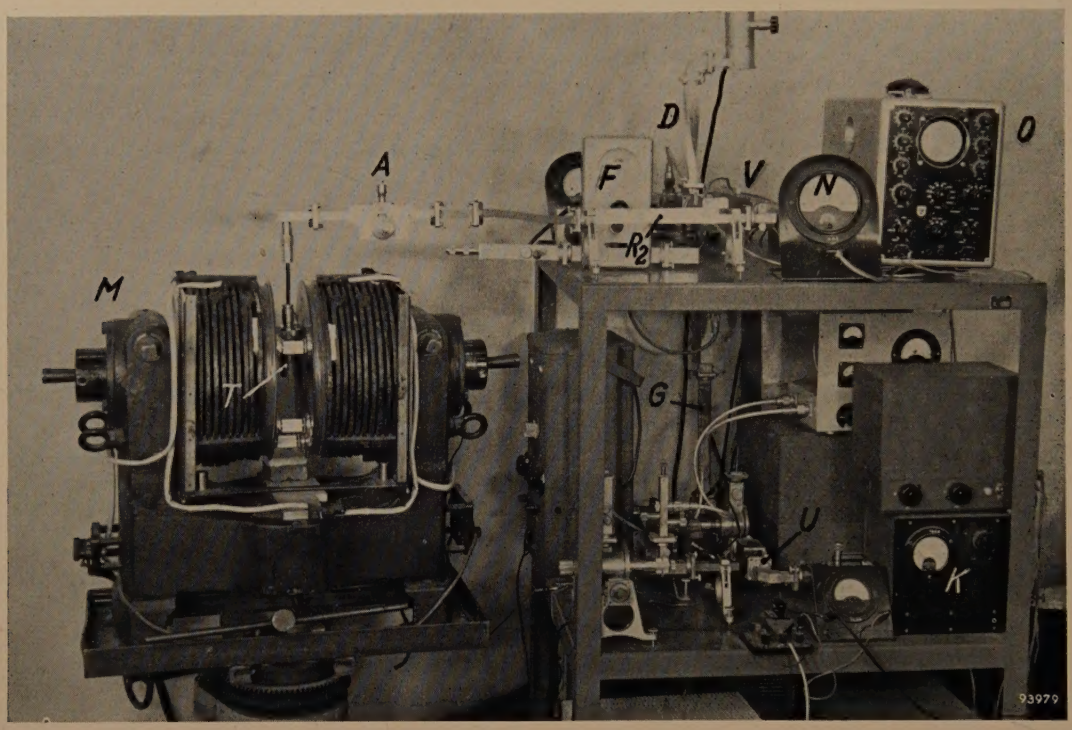

Fig. 4. Set-up used in the Philips laboratory at Eindhoven. *O* is an oscillograph. Other letters as in fig. 3.

For studying a given resonance spectrum the total width Δf of the spectrum (B remaining constant) or the corresponding width ΔB (f remaining constant) should be small with respect to the average value of f or B respectively. As already pointed out, this is why it is necessary (apart from the intensity of the phenomenon) to work with high frequencies and hence also with strong fields. In most cases the average value chosen for B is between 0.02 and 2 Wb/m^2 [200-20 000 gauss], the corresponding frequencies being 6×10^8 c/s and 6×10^{10} c/s ($\lambda = 50$ cm and 0.5 cm respectively). The preferred wavelengths are $\lambda = 1.25$ or 3 cm. Shorter waves and stronger fields are too difficult to produce experimentally to be suitable for day-to-day investigations.

range of components with which it is possible to build apparatus as in fig. 3 for frequencies up to 10 000 Mc/s.

Paramagnetic resonance spectra of Mn^{2+} in solids

As discussed in the introduction, paramagnetic resonance generally occurs not at a single frequency f_r, but in a certain frequency range in the neighbourhood of this frequency. A spectrum is found which has several components, each of which has a specific width and may also have an individual structure.

Let us now examine how this splitting process and broadening of the components come about. We have hitherto assumed that all atomic magnets (e.g. the resultant of the spins of the electrons of one ion) are subjected to the same field, namely to the

external field B. Frequently the atomic magnets are subjected not only to the field B but also to an extra field b, the origin of which is discussed below. According to (1) and (5) we know that resonance then occurs if [10])

$$f = g\frac{e}{4\pi m}(B+b), \quad . \quad . \quad . \quad (10a)$$

i.e.,

$$B = \frac{f}{ge/4\pi m} - b. \quad . \quad . \quad . \quad . \quad (10b)$$

The field b, and therefore the shift in the resonance spectrum, may not be the same for all the resonating atomic magnets, so that splitting or broadening of the lines may occur.

Assume for the sake of simplicity that the atomic magnet is a paramagnetic ion, whose paramagnetism arises from a single electron. The extra magnetic field b to which this electron is subjected may have several causes. We shall consider three of them:

a) the field due to a magnetic moment of the atomic nucleus;
b) fields due to neighbouring paramagnetic ions;
c) fields due to the movement of the electron through the electrostatic field of the crystal lattice (caused by nuclei and electrons).

[10]) The suffix to the symbol g will now be dropped since the electrons in a crystal lattice have a value of g (generally ≈ 2) which may differ from the value $g_e = 2.0023$ for a free electron.

In the following we shall deal first with a special case, that of divalent manganese ions (Mn^{2+}) dispersed randomly in a crystal lattice. We shall then go on to examine other applications of the investigation of paramagnetic resonance.

Effect of nuclear spin; hyperfine structure

The Mn^{2+} ion contains five electrons in an incompletely occupied electron shell, so that $S = \frac{5}{2}$ (in the ground state). If these electrons were subjected solely to the influence of the external field B, there would be six equidistant energy levels, the distance between which would be proportional to B. A representation of these energy values is given in *fig. 5a*. Resonance occurs according to (4) when $hf = \Delta E$, where f is the constant frequency of the klystron. Since the energy levels are equidistant, this condition is fulfilled for all transitions by one and the same value of B. Consequently the resonance would occur at only one value of B, and the spectrum would consist of a single absorption line, as represented below in fig. 5*a*.

In reality the situation is more complicated, since the nucleus of the manganese atom also has a magnetic moment. Manganese consists of only one stable isotope, the mass number of which is 55. The nucleus of this isotope has a spin given by its spin number $I = \frac{5}{2}$. The corresponding magnetic moment is $3.461(e/2m_p)(h/2\pi)$, where m_p represents the proton mass. The electrons that contribute to the para-

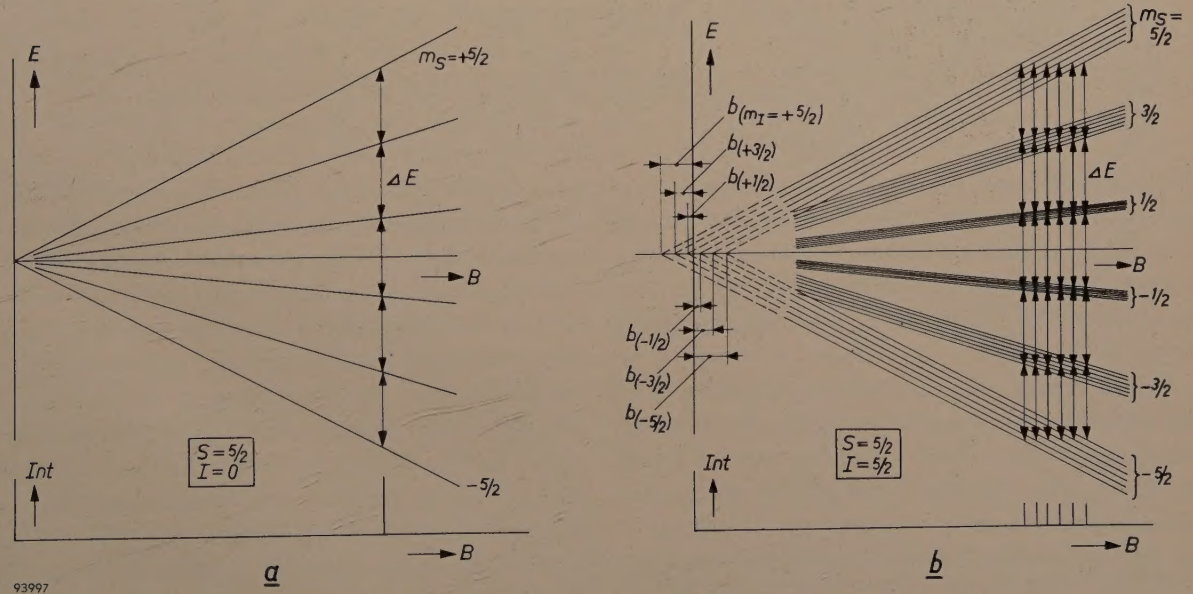

Fig. 5. *a*) Energy-level scheme of an ion with $S = \frac{5}{2}$ in a magnetic field B; below, the resulting resonance spectrum (intensity *Int* as a function of B), which in this case consists of a single line.
b) The same for an ion with $S = \frac{5}{2}$ which moreover has a nucleus of spin number $I = \frac{5}{2}$ (Mn^{2+}). Each of the levels of (*a*) is split into six sub-levels, corresponding to the six values of the field $B+b$. The 30 possible transitions give rise to six resonance peaks, as shown below.

magnetism are subjected both to the influence of the external magnetic field and to that of the nuclear field. Now, in a manner analogous to that described for electrons, a nucleus with spin number I has altogether $2I + 1$ possible positions with respect to the field B. As a result, the parallel component b of the extra nuclear field, which acts on the electrons, also has $2I + 1$ possible values. Each of the $2S + 1$ levels of the paramagnetic ion is thus split into $2I + 1$ levels (fig. 5*b*). Since $S = \frac{5}{2}$ and $I = \frac{5}{2}$, this gives $6 \times 6 = 36$ levels. Since transitions occur only between the adjacent levels of fig. 5*a*, there are in all $6 \times 5 = 30$ transitions between the split levels of fig. 5*b*, the energy differences relating to any one value of b being equal. In consequence of this the resonance condition is now fulfilled for six values of B, so that the resonance line in fig. 5*a* is in reality split into six components, as illustrated below in fig. 5*b*.

smaller is the splitting. A study of this splitting process therefore yields information on the spatial distribution of the electrons.

This, of course, provides information only on those electrons belonging to the outer, non-closed electron shells, for the electrons in closed shells do not contribute to the paramagnetism. Now it is precisely for the outer-shell electrons that the extent of the orbits, and hence the average field to which they are subjected by their "own" nucleus, is affected by the environment of the ion. Paramagnetic resonance can therefore also provide information on this environment. *Fig. 6* shows the paramagnetic resonance spectra of Mn^{2+} ions incorporated in different crystal lattices [12]). All these crystals contain divalent ions. A small fraction of these (0.1—0.01%) are replaced by Mn^{2+} ions. It can be seen from fig. 6 that the splitting of the resonance

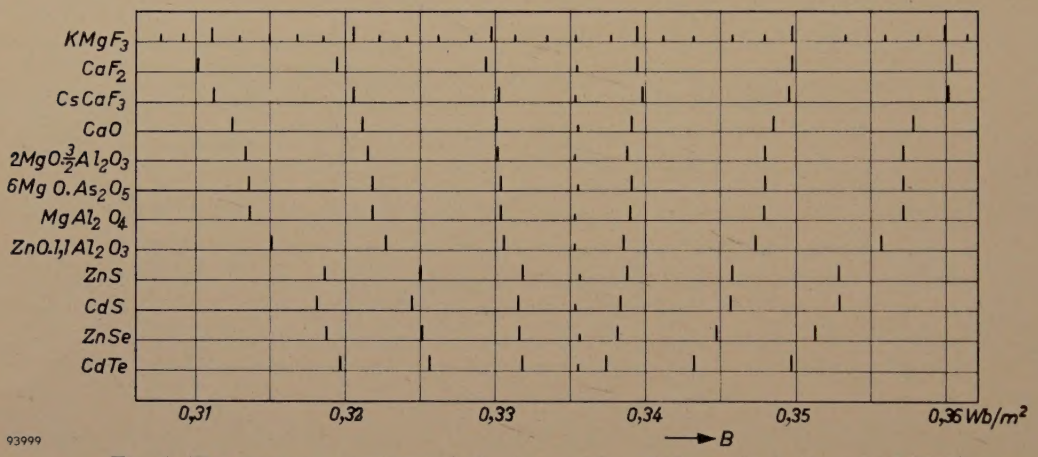

Fig. 6. The resonance spectrum (only the *position* of the peaks is shown) of Mn^{2+} in various crystal lattices. The magnitude of the splitting depends mainly on the nature of the negative ion.

This splitting into components (hyperfine structure [11])) occurs in many other ions besides the example given of Mn^{2+}. (About half the stable isotopes of all elements possess a nuclear spin.) The magnitude of the splitting is determined by the average field excited by the atomic nucleus at the position of the electrons involved in the resonance. This average field depends on the nature of the nucleus and on the extent of the electron orbit: the further away the electron is from the nucleus, the line of Mn^{2+} does, in fact, differ considerably in different environments. From the results of measurements on three different fluorides ($KMgF_3$, CaF_2 and $CsCaF_3$), and on two sulphides (CdS and ZnS), of widely differing lattice constants, it appears that the latter play hardly any role in this process. The magnitude of the splitting is almost entirely determined by the nature of the negative ions surrounding the Mn^{2+} ions. With F, O, S, Se and Te the average magnitude of splitting in the B spectrum is respectively 98, 80-90, 69, 65 and 59×10^{-4} Wb/m^2.

Now it is known that in the above series of compounds (fluorides, oxides etc.) the bond is the most ionic in nature in the fluorides, and that in the order given it becomes gradually more homopolar

[11]) In the theory of atomic spectra the term fine structure is used when referring to a multiple spectral line (e.g. the D_1D_2 doublet of sodium) produced by the splitting of an energy level as a result of *spin-orbit* interaction; the term hyperfine structure relates to a multiplet produced by interaction with the *nuclear spin*. The hyperfine structure is generally small as compared with the normal fine structure. In the case of paramagnetic resonance this terminology is retained although, here, the effect of the nuclear spin may be large compared with other effects.

[12]) J. S. van Wieringen, Paramagnetic resonance of divalent manganese incorporated in various lattices, Disc. Faraday Soc. **19**, 118-126, 1955.

in nature. The case of the more homopolar compounds can be characterized by saying that the outermost electrons of the cation (Mn^{2+}) are partly associated with the electron clouds in the surrounding anions, and thus, on an average, are farther away from the Mn nucleus. The differences in the magnitude of the splitting in fig. 6 are accordingly in good agreement with what was known qualitatively of the nature of the bond between the ions of the series listed above, and moreover have provided useful quantitative information.

It can be seen from this that the study of the structure of paramagnetic resonance lines is a valuable tool in investigations into the nature of the bonding in crystals. It is used in an analogous way to analyse the bonds in complex molecules: the unsaturated bond present in a free radical, which functions as an atomic magnet, has been localized near certain atoms in the radical in many cases by studying the paramagnetic resonance spectrum.

Effect of the magnetic fields of neighbouring paramagnetic ions; line broadening

Apart from the external magnetic field, and possibly the field of the nuclear spins, another field may be operative: this is the field originating from neighbouring paramagnetic ions, particularly from those of the same kind as the resonating ion. This field also contributes to the term b in the resonance condition (10). Since, however, it originates from a large number of similar ions, which all occupy different attitudes in space and are at different distances from the ion concerned, the result in this case is not a splitting into a relatively small number of lines (as in the case of the nuclear spin), but a splitting into so many components that only a broadening of the resonance line is observed. The greater the concentration of the paramagnetic ions, the smaller is their average distance from each other and the stronger are the magnetic fields they exercise on their neighbours, and hence the greater is the broadening of the resonance line. This can be seen from *fig. 7*, which shows the paramagnetic resonance spectrum of Mn^{2+} added to ZnS, for varying percentages of manganese [13]). With increasing manganese content the spectrum changes from six more or less separate lines into a single broad maximum, exhibiting very little structure. This is also the reason why it is, in general, not possible to separate the resonance spectrum into components in a pure compound of paramagnetic ions (e.g. MnS). The components only become visible when the paramagnetic ions have been strongly diluted by the admixture of non-magnetic ions, such as Zn^{2+} (see fig. 7).

Effect of electron motion in the electrostatic crystalline field

The influence of the crystalline field becomes manifest in a splitting of the energy levels, which appears even in the absence of an external magnetic field. A proper analysis of this phenomenon involves rather complicated and detailed considerations, which cannot be pursued here. It will be enough for our purposes to discuss merely the broad outlines.

It was assumed in the foregoing that the magnetic moment of atomic magnets (i.e. in our case the Mn^{2+} ions) is due solely to electron spins. This assumption is not of general validity, since the orbital motion of the electrons also contributes to the magnetic moment. In the case of free paramagnetic ions and atoms the magnetic moment is the resultant of a spin and an orbital moment which are of the same order of magnitude.

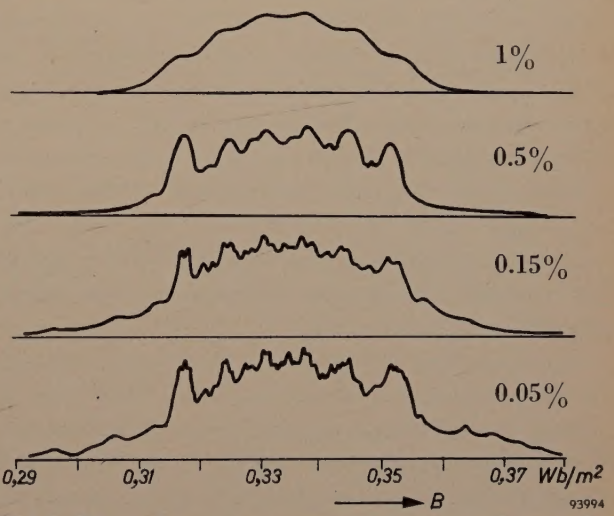

Fig. 7. Effect of the paramagnetic ion concentration on the spectrum. The spectrum of hexagonal ZnS (wurtzite) with the addition of various amounts (atom %) of Mn.

A paramagnetic ion or atom in a crystal lattice, however, is subjected to strong electrostatic fields. This has two important effects on its magnetic properties. In the first place the orbital moment is almost entirely destroyed, because the electrons move in their orbits in different directions (a quantum-mechanical effect, described in small print below) and this makes the resultant orbital current vanishingly small. The magnetic moment of the ion (and the same applies to electrons in paramagnetic centres) is therefore identical with the spin moment. This fact has already been employed in the deriva-

[13]) J. S. van Wieringen, Influence du traitement mécanique sur la résonance paramagnétique du manganèse dans les poudres de sulfure de zinc, Physica **19**, 397-400, 1953.

tion of formula (5). If, however, we wish to consider the situation more precisely, we must take into account the presence of a certain field due to the orbital moments, which causes the total magnetic moment of the incorporated ion to differ somewhat from the spin moment. Consequently the factor g_e (= 2.0023) in (5), which applies to a free electron, must be replaced by another factor g. This causes a shift in the field B at which resonance occurs; see equations (1) and (10), in which this is taken into account.

The second effect of incorporating the ion in a crystal lattice is that the orbital moment, in so far as it is still present, becomes anchored to the electrostatic field of the crystal. It can therefore no longer move freely in space, unlike the spin moment, which is almost entirely free. The spin moment is, however, only weakly coupled to the orbital moment by the spin-orbit interaction; the coupling with the crystal lattice is therefore small.

Owing to the orbital motion being bound to the crystalline field, the contribution of the residual orbital moment to the total magnetic moment of the atomic magnet depends as a rule on the orientation of the crystal in the external field B. The spectrum is therefore also dependent on this orientation; in other words, the paramagnetic resonance spectrum is not, generally speaking, isotropic with respect to the external field. The magnitude of the difference between g and g_e, and the symmetry of the anisotropy depend on the strength and the symmetry of the crystalline field and on the structure of the ion or atom (or other centre) functioning as atomic magnet.

We now come to the earlier mentioned splitting of the paramagnetic resonance lines which may be caused by the crystalline field. Spin-orbit interaction is a consequence of the motion of the electron in the electric field of the crystal lattice giving rise to a local magnetic field at the position of the electron (this field attempts to orient the magnetic moments of spin and orbit in opposite directions). The other electrons and nuclei in the lattice are in a state of motion with respect to the electron concerned, and therefore function as electrical currents which give rise to a magnetic field. This extra magnetic field can be taken into account, as in (10), by adding a field b to the external field B. The strength of the spin-orbit interaction, hence the magnitude of b, depends on the angle between the spin moment and the orbital moment. It may therefore vary for different spin orientations, and moreover it again depends on the attitude of B with respect to the crystalline field. Spin-orbit interaction, then, can give rise to line splitting, the magnitude of which depends on the orientation of the crystal in the external magnetic field (and again, of course, on the structure of the ion, atom or other centre acting as atomic magnet); see *fig. 8*.

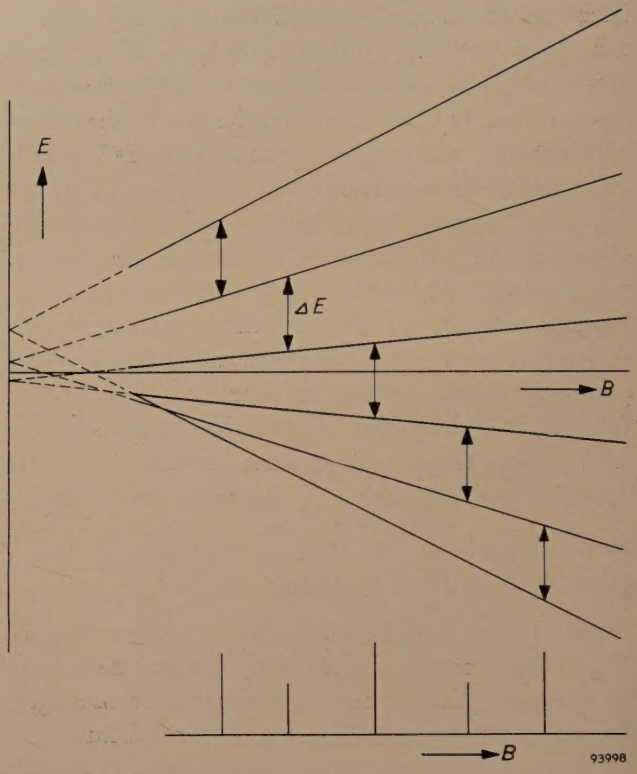

Fig. 8. Illustrating the effect of electron motion in the electrostatic field of the crystal. In a non-cubic crystal different orientations of the spin with respect to the crystallographic axis correspond to different energies. In the case of $S = \frac{5}{2}$ there are three energy levels, corresponding to $m_s = \pm\frac{1}{2}, \pm\frac{3}{2}, \pm\frac{5}{2}$. In a magnetic field each of these levels is split into two. Below, the resultant resonance spectrum (five lines). The effect of nuclear spin is neglected here.

This line splitting is only possible when the spin number of the atomic magnet is greater than $\frac{1}{2}$. Where the spin number is $\frac{1}{2}$ there are only two levels and only one transition can take place between them, and therefore no splitting pattern can appear. Larger spin values can give rise to a complicated spectrum.

The magnitude of the splitting depends not only on the attitude of the crystal in the magnetic field but again on the nature of the crystalline field in which the ion is situated. The lower the symmetry of the crystalline field the greater the splitting. For cubic crystals the splitting is very often zero, or at least very small.

We shall illustrate this with an example [13]), again taking the Mn^{2+} ion. *Fig. 9a* shows the resonance spectrum of wurtzite (hexagonal ZnS) to which a small percentage of Mn (0.05 percent) has been added. The spectrum is a very complicated one. The cubic modification of ZnS (sphalerite) shows the

simple spectrum with six hyperfine-structure components, fig. 9*e*. Now the paramagnetic resonance spectrum of Mn in hexagonal ZnS is found to change considerably when the specimen is deformed. This can be seen from fig. 9*b*, *c*, *d*, which show the spectrum after compression of the specimen at different

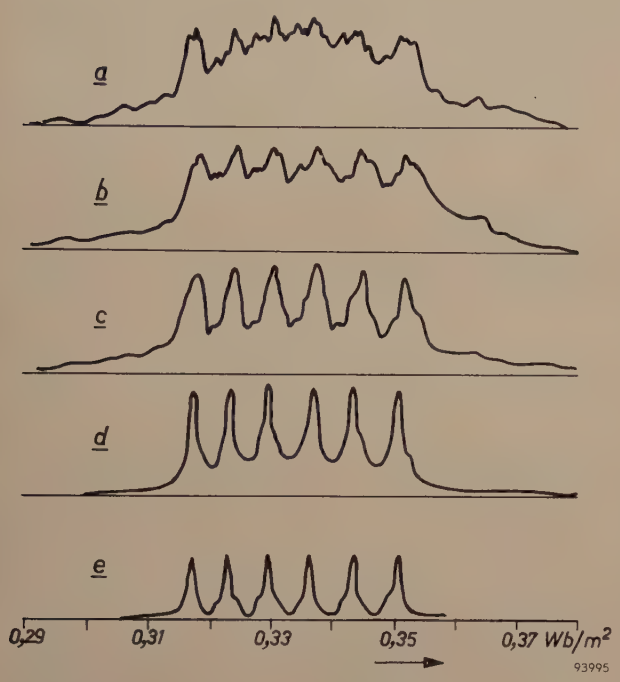

Fig. 9. Example of how the symmetry of the crystal lattice affects the resonance spectrum. In *a*) and *e*) are shown the resonance spectra of Mn^{2+} (0.05%) in wurtzite (hexagonal ZnS) and in sphalerite (cubic ZnS), respectively. The other spectra show how, under an applied pressure, the crystal structure changes from hexagonal to cubic. The relevant pressures were: *b*) 750 kg/cm², *c*) 1500 kg/cm², *d*) 3500 kg/cm².

pressures. The spectrum gradually changes during this process to that of cubic ZnS. The explanation of this phenomenon is that hexagonal ZnS is metastable at room temperature. The cubic structure represents the stable state. A relatively small pressure is sufficient to convert the hexagonal form into the stable cubic form; the conversion is more complete the higher is the pressure, more crystals then changing from the hexagonal to the cubic form. This process can be followed closely by studying the paramagnetic resonance of incorporated Mn.

The transition from the hexagonal to the cubic lattice is demonstrated by a crystal model in *fig. 10*.

It is instructive to examine how the quantum-mechanical description accounts for the effect of the crystalline field on the orbital moment. We shall start from the quantum-mechanical explanation of the bonding in the hydrogen molecule ion H_2^+.

With this ion the electron is associated now with the one and now with the other hydrogen nucleus. If we represent this by two wave functions ψ_1 and ψ_2, we can combine these into a symmetrical function $\psi_1 + \psi_2 = \psi_s$ and an anti-symmetrical function $\psi_1 - \psi_2 = \psi_a$. The chance of an electron being found at a particular point in space is given by $|\psi|^2$ at that point. In the case of ψ_s the most probable position of the electron is between the two nuclei, for ψ_a the most probable position is outside them. If the nuclei are widely spaced, the energy of both wave functions is equal ($E_s = E_a$). If the distance between the nuclei is decreased, then $E_a > E_s$ and the symmetrical wave function represents the energetically more favourable state. The effect of introducing a perturbation in the form of an external electrical field which exerts a force on the electron, e.g. parallel to the line connecting the nuclei, and directed from nucleus 2 to nucleus 1, is to change the wave functions in this field. The energetically more favourable wave function can now be represented approximately by a linear combination of the original ψ_s and ψ_a:

$$\psi = A\psi_s + B\psi_a,$$

where $A \gg B$. It is said that the function ψ_s is mixed with a little of ψ_a. The result of this is that ψ_1 and ψ_2 in the expression for $|\psi|^2$ no longer occur symmetrically, which can be interpreted by saying that there is now a greater probability of finding the electron near nucleus 1 than near nucleus 2. The external field "blows", as it were, the electron towards nucleus 1.

Something of the kind occurs when a paramagnetic ion is placed in a crystalline field. If by ψ_1 and ψ_2 we now understand wave functions corresponding respectively to an anti-clockwise and clockwise motion of the electron, we again have the combinations ψ_s ($= \psi_1 + \psi_2$) and ψ_a ($= \psi_1 - \psi_2$). One of these is energetically more favourable, because the spatial distribution of the electron it represents is more favourable with respect to the crystalline field. The orbital moments corresponding to both ψ_s and ψ_a are zero (i.e. anti-clockwise and clockwise motion are equally probable). The spin-orbit interaction remains, however. It has the character of a perturbation, which gives rise to another energetically most favourable state, for which the wave function is again approximately given by $A\psi_s + B\psi_a$, where, e.g., $A \gg B$; in other words, there is again a mixing of wave functions. The result is that ψ_2, for example, prevails over ψ_1. The probability of clockwise motion of the electron is then greater than that of anti-clockwise motion, and therefore a residual orbital moment exists.

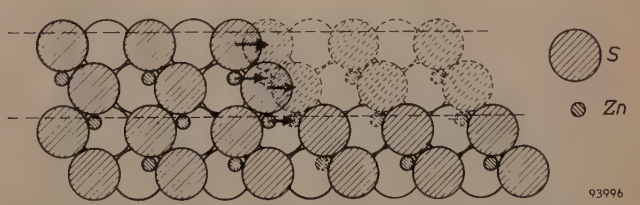

Fig. 10. Cross-section of a crystal of hexagonal ZnS parallel to a plane containing the hexagonal axis and a two-fold axis (left half of diagram) and cross-section of face-centred cubic ZnS crystal parallel to a (110) plane (right). Both lattices are close-packed structures of sulphur ions. The tetrahedral sites are occupied by zinc ions. The sulphur and zinc ions lie in layers perpendicular to the plane of the drawing. A comparison of the left and right sides shows that the bottom and next-to-bottom layers in the figure are identical. The difference between the hexagonal and the cubic structure appears in the third layer from the bottom.

Under the influence of an applied pressure (at room temperature) hexagonal ZnS changes to cubic ZnS. This occurs by a glide process, in which each third layer glides over the one immediately below it. The drawing shows two glide planes (dashed lines). The arrows represent ion displacements during the glide process.

Since in this case the energy difference between the states ψ_s and ψ_a is of the order of 0.1 eV, and the spin-orbit interaction of the order of 0.001 eV, the perturbed state lies very close to the state of zero orbital moment. The resultant orbital moment is therefore always very small compared with that of a free atom or ion.

A particle that simultaneously rotates anti-clockwise and clockwise (with almost equal probabilities of either) corresponding, for example, to the function ψ_s, is of course unthinkable in classical mechanics. This is a typical illustration of the fact that the behaviour of electrons in atoms and ions is entirely different from that of macroscopic particles, and can be described only in terms of quantum mechanics.

Let us now briefly summarize the information that can be deduced from the investigation of paramagnetic resonance spectra.

The *magnitude* of the resonance absorption generally indicates the number of atomic magnets in the substance investigated.

From the *displacement* of the resonance spectrum (difference in g value) the orbital contribution to the magnetic moment can be deduced. With single crystals the anisotropy (with respect to the field) of the displacement provides information on the symmetry properties of the crystal lattice in the immediate neighbourhood of the atomic magnet.

The *line width* — if caused by atoms or ions of the same kind — yields information on the mutual spacing of the atomic magnets.

Line-splitting can have several causes. So-called hyperfine structure is an effect of nuclear spin, while so-called fine structure is due to the crystalline field. We can distinguish between these two possibilities by observing the ratio of intensities of the line components. In the case of hyperfine structure, the number of components provides information on the nucleus of the atomic magnet (or on the nuclei in the immediate vicinity). The magnitude of the splitting allows deductions to be made regarding the spatial distribution of the electrons of the atomic magnet concerned, and possibly regarding the inter-atomic bonds. If, on the other hand, the splitting is caused by the crystalline field, it tells us something about the spin of the atomic magnet and (in single crystals) about the symmetry of the local crystalline field.

Other investigations of paramagnetic resonance

Apart from the investigations described above, which relate to Mn^{2+} ions, we shall now describe a few other interesting cases, some of which have been examined in this laboratory.

F centres of alkali-halides

Alkali-halides (NaCl, KCl, etc.), when subjected to X-radiation, show an absorption band in or near the visible part of the spectrum. KCl, for example, becomes violet because an absorption band is produced in the green. It has been found from various experiments that this absorption band is attributable to a halogen ion being replaced by an electron on some lattice sites [14]). These sites are called F centres. An old dispute in this connection concerned the question of how strongly the electron is localized. Does it remain inside the vacancy left by the halogen ion or is it distributed over the six surrounding positive alkali ions?

This dispute was settled by experiments carried out by Kip, Kittel, Levy and Portis [15]). Since the F centre contains a single electron, it is paramagnetic. It exhibits paramagnetic resonance, having a spectrum, as expected, consisting of one line. One of the observables is the displacement of the line, from which it follows that, for KCl, $g = 1.995$ (against $g_e = 2.0023$ for free electrons). This points to a relatively large moment, which can be better explained by the dispersed model than by the localized one. An additional confirmation of the dispersed model follows from the line width, which is too large to be explained in terms of the magnetic interaction of centres dispersed at random over the lattice. At first it was deduced from this that the F centres occurred in clusters. It later appeared, however, that the line width was caused by the electron interacting not only with the six nearest-neighbour alkali nuclei but also with the twelve next-nearest-neighbour halogen nuclei. Since there are so many nuclei involved, the interaction in this case does not lead to a clearly visible hyperfine structure, but to a line broadening with unresolved separate components. The fact that the broadening in this case is caused by interaction with nuclear spins was convincingly demonstrated by making use of other alkali isotopes. These have a different nuclear spin and a different interaction. It was possible to give a quantitative explanation of the different line width then observed.

Centres in irradiated quartz crystals

Griffiths, Owen and Ward [16]) found paramagnetic resonance in quartz crystals subjected to X-radiation. The resonance line showed a hyperfine struc-

[14]) J. H. de Boer, Electron emission and adsorption phenomena, Univ. Press, Cambridge 1935. See also E. J. W. Verwey, Electronic conductivity of non-metallic materials, Philips tech. Rev. **9**, 46-53, 1947/48.

[15]) C. A. Hutchison, Phys. Rev. **75**, 1769, 1949.
A. F. Kip, C. Kittel, R. A. Levy and A. M. Portis, Phys. Rev. **91**, 1066, 1953.
N.W. Lord, Phys. Rev. **105**, 756, 1957 (No. 2).

[16]) J. H. E. Griffiths, J. Owen and I. M. Ward, Nature **173**, 439, 1954.
Mary C. M. O'Brien, Proc. Roy. Soc. London A **231**, 404, 1955.

ture of six lines, and the resonance field B was found to depend on the attitude of the crystal in the external magnetic field (anisotropy of g). The hyperfine structure appeared to be due to aluminium. The investigation led to the conclusion that the centres formed were localized at Al ions which occur as impurities in SiO_2. The examination of the anisotropy showed that the charge cloud of the centre is oriented along the lines connecting oxygen atoms. A detailed description has been given by Mary O'Brien.

Donors and acceptors in semiconductors

Some crystalline substances, such as Si and SiC which are almost perfect insulators in the pure state, can be made into semiconductors by the addition of a very small percentage of donors or acceptors, i.e. foreign atoms which either give up an electron to the crystal lattice or absorb an electron from the lattice (in the latter case conductivity is obtained by displacement of the electron hole in the lattice). At very low temperatures, the electron or the electron hole does not leave the donor or the acceptor, as the case may be, but remains localized in its vicinity. For this experiment Si must be placed in liquid helium (—269 °C) [17]) and SiC in liquid nitrogen (—190 °C) [18]). In that state the donor or the acceptor atoms are generally paramagnetic. This appears from the occurrence of a paramagnetic resonance line, in which, moreover, a hyperfine structure is found. At higher temperatures this line vanishes, because the electrons or holes are then released from the donors or acceptors and are able to move more or less freely through the lattice. Resonance without hyperfine structure may then occur, as in fact has been observed in the case of Si.

Summary. After a brief description of the phenomenon of paramagnetic resonance, the quantum-mechanical theory of the phenomenon is discussed. Reference is made to the relation between paramagnetic resonance and the Zeeman effect, and to the relationship with ferromagnetic resonance in ferromagnetics. For observing paramagnetic resonance use is made of a resonant cavity, containing the substance under investigation and attached to a waveguide through which radiation of constant frequency is passed (e.g. $\lambda = 3$ cm), the cavity being placed in a constant magnetic field. The strength of this field is varied and the signal reflected from the resonant cavity is detected and recorded as a function of the field strength. This reveals a spectrum which usually shows several peaks, each of which has an individual structure. An extensive investigation has been made of the spectrum in the case of divalent manganese, Mn^{2+}, in various crystal lattices. Six components are usually found (hyperfine structure due to nuclear spin). The influence of the bonding in the crystal lattice (competition between ionic and homopolar bonding), of the manganese content (neighbouring ions) and of the symmetry of the crystal lattice (hexagonal and cubic ZnS) are discussed in the light of the experimental results. Mention is then made of some other results of paramagnetic-resonance investigations, namely the resonance of F centres of alkali-halides, of centres in irradiated quartz crystals and of donors and acceptors in semiconductors. The examples chosen give some idea of the information that can be derived from paramagnetic resonance spectra.

[17]) R. C. Fletcher, W. A. Yager, G. L. Pearson and F. R. Merritt, Phys. Rev. **95**, 844, 1954.
A. M. Portis, A. F. Kip, C. Kittel and W. H. Brattain, Phys. Rev. **90**, 988, 1953.

[18]) J. S. van Wieringen, Internationales Kolloquium über Halbleiter und Phosphore, Garmisch-Partenkirchen, 1956; to be published by F. Vieweg, Brunswick 1958.

AN X-RAY DIFFRACTION TUBE WITH ROTATING ANODE FOR 10 kW CONTINUOUS LOADING

621.386.26:548.73

X-ray tubes for use in diffraction analysis are usually of the sealed-off type, the anode being fixed and water-cooled. If such a tube has a copper anode and a true focus measuring 10 mm², say, it will be capable of taking a maximum power load of round about 1 kW. If other materials are used for the anode and the design otherwise remains unchanged, the maximum power will not be more than a few hundred watts.

For those kinds of diffraction analysis that may call for extremely long exposure times, it is of advantage to have tubes of much higher ratings available. An example of such work that comes immediately to mind is the study of certain phenomena by means of the *diffuse* scattering. One important type of investigation coming under this head is that into the kind of movement performed by certain atomic groups in some crystals when the temperature rises above a certain value (for example, the NO_3 radical in $NaNO_3$ starts rotating as the compound passes into the modification stable at high temperatures). The structure of mixed crystals also gives rise to diffuse scattering which is sometimes measurable (e.g. in NaCl-KCl). Another field in which the investigator is concerned with low intensities is the analysis of albumin structures.

Higher power ratings can be obtained by arranging for the water-cooled anode to rotate. Only a small number of X-ray diffraction tubes with a rotating water-cooled anode have been constructed [1]). A tube of this kind has been built in the Philips laboratories at Eindhoven in order to gain experience in the various design problems involved. The tube has a copper anode — copper radiation is the most commonly used in diffraction analysis — and can take a continuous load of 10 kW (40 kV at 250 mA). It is very compact in construction.

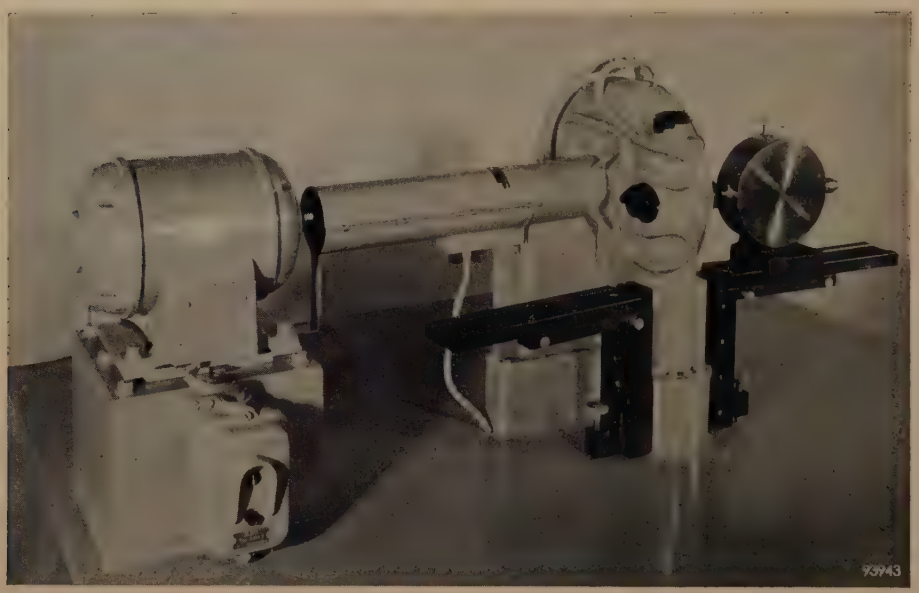

Fig. 1. A rotating-anode X-ray diffraction tube built in the Philips laboratories at Eindhoven; the rotating water-cooled anode can take a continuous load of 10 kW. The motor is on the left, the housing accommodating the anode disc is on the right, and on the extreme right, mounted on a slide, is an X-ray diffraction camera.

Fig. 1 is a view of the exterior of the tube. On the left is a three-phase motor, which drives the anode (at 920 r.p.m.) via a shaft with a universal joint; the housing in which the anode disc is accommodated is on the right, and on the extreme right is a camera mounted on a slide. There is also a camera slide on the motor side of the housing.

The focus is formed on the outer edge of the anode disc and has dimensions 1 mm × 10 mm (*fig. 2*). Three beryllium windows, 1 mm thick, allow the passage of radiation to the exterior; they are mount-

[1]) A. Müller, Brit. J. Radiol. **4**, 127, 1931.
R. E. Clay, Proc. Phys. Soc. **46**, 703, 1934.
A. Taylor, J. sci. Instr. **26**, 225, 1949.
W. T. Astbury, Brit. J. Radiol. **22**, 360, 1949.
E. A. Owen, J. sci. Instr. **30**, 393, 1953.

ed in black frames that may be distinguished in fig. 1. Through two of the windows the radiation leaves the housing in a horizontal direction; from the third it is beamed vertically upwards. Since the

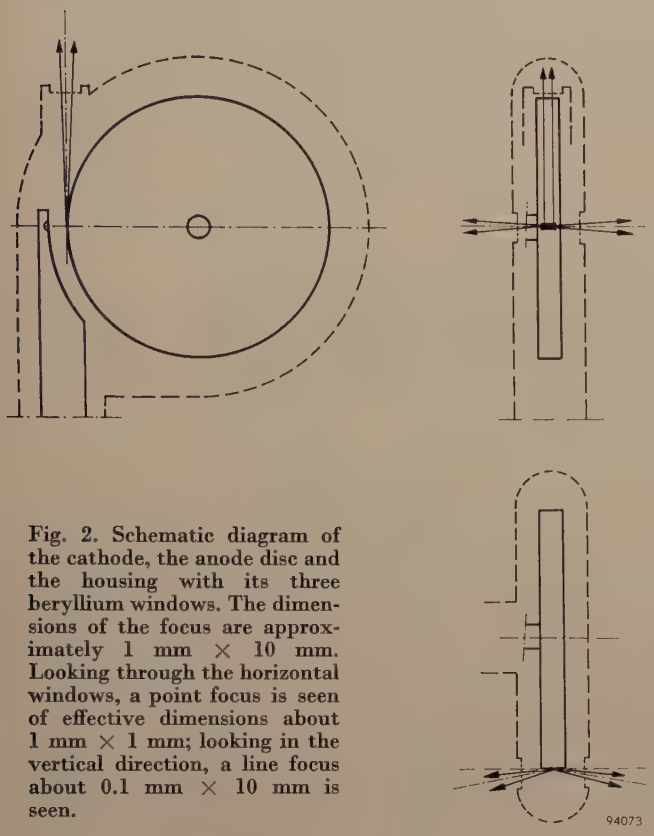

Fig. 2. Schematic diagram of the cathode, the anode disc and the housing with its three beryllium windows. The dimensions of the focus are approximately 1 mm × 10 mm. Looking through the horizontal windows, a point focus is seen of effective dimensions about 1 mm × 1 mm; looking in the vertical direction, a line focus about 0.1 mm × 10 mm is seen.

slides are almost parallel with the axis of the disc (at an angle of 6° to this axis), a point focus of approximately 1 mm × 1 mm is presented to the camera; looking through the upper window, one sees a line focus [2]) of approximately 0.1 mm × 10 mm. The windows can be covered on the outside by small lead shutters.

Fig. 3 shows a vertical section through that part of the tube containing the shaft and the anode disc. The plane of the drawing passes through the axis of the shaft (*A-A*). The housing is made up of a fixed portion *C* and a removable circular cover *E*. Removal of the cover allows the anode disc *D* and the shaft to be extracted from the housing for cleaning and maintenance purposes.

The shaft turns in ball-bearings (B_1 and B_2) and passes through five tight-fitting rings (numbered *1-5*) made of a synthetic rubber that is proof against oil and heat. These rings have an internal metal reinforcement, and they fit closely round the shaft and round the inside of the housing, so that they divide the enclosed space into a series of chambers.

Throughout that part of its length marked *a-a*, the shaft consists of two co-axial cylinders. The cooling water entering at inlet *F* passes into the chamber formed by rings *4* and *5*, and penetrates thence through holes *f* into *L*, the inner cylinder. From there the water flows through three radial pipes inside the disc into a runnel *J* which underlies the anode strip *K* throughout the periphery of the disc. The return path is via three other radial tubes into *H*, an annular space between the two cylinders just referred to; the water finally leaves the tube by way of holes *g*, the chamber formed by rings *3* and *4*, and outlet *G*. A high vacuum exists in the large compartment to the right of ring *1*, which makes a vacuum-tight fit around the anode shaft. The chamber between rings *1* and *2*, which contains ball-bearings B_1, leads to a vacuum reservoir connected to the backing pump. That between rings *2* and *3* separates the vacuum space from the cooling-water chamber, and serves to drain off any water that may leak through ring *3*.

Since the part of the housing in the vicinity of the focus is subjected to secondary-electron bombardment while the tube is in operation, it must also be cooled: this is necessary above all to protect the various rubber rings that serve as vacuum seals for the windows etc. The power to be dissipated from the housing when the tube is under full load is about

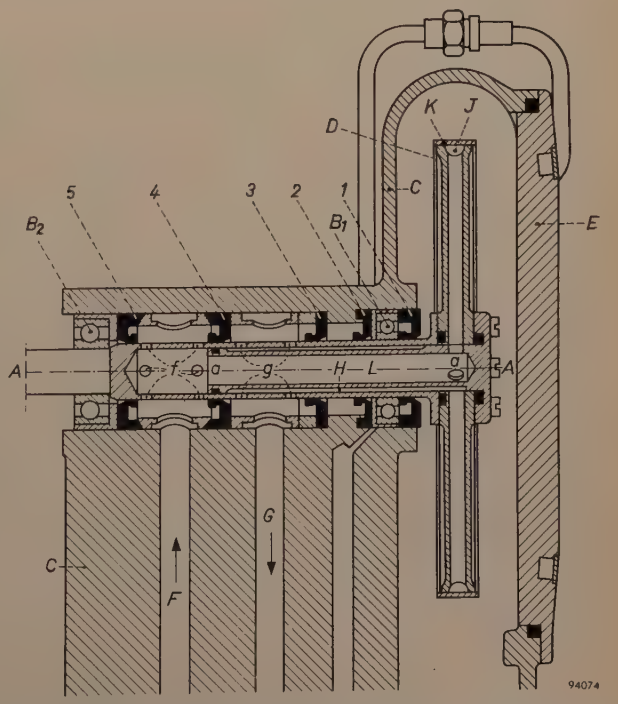

Fig. 3. Vertical section through the housing, the shaft and the anode disc. The drawing shows the bearings, seals and water-cooling arrangements for the rotating anode (one or two non-essential features have been omitted).

[2]) The use of the point focus and of the line focus is discussed in J. E. de Graaf and W. J. Oosterkamp, Philips tech. Rev. **3**, 259, 1938.

1 kW. The cooling-water pipes fixed to the exterior of the housing may be seen in fig. 1.

A centrifugal switch mounted on the shaft cuts off the anode tension whenever the disc stops turning, whatever the reason. The switch is mounted inside the cylindrical housing, between the motor and the X-ray tube housing (see fig. 1).

The cathode assembly has a tungsten filament 0.3 mm thick, fixed to the lead-in wires by means of two small screws; it can therefore be changed very quickly. The life of the filament is about 200 hours. The cathode assembly is inserted into the tube from below, a vacuum-tight closure being made by means of a flanged screw-cap and a rubber ring. Part of the porcelain insulator carrying the supply leads to the cathode can be seen in the general view of *fig. 4* (owing to the mechanical design of the tube the anode has to be at earth potential, and hence the cathode assembly is at high tension). Beneath the insulator is a black metal sphere that serves to

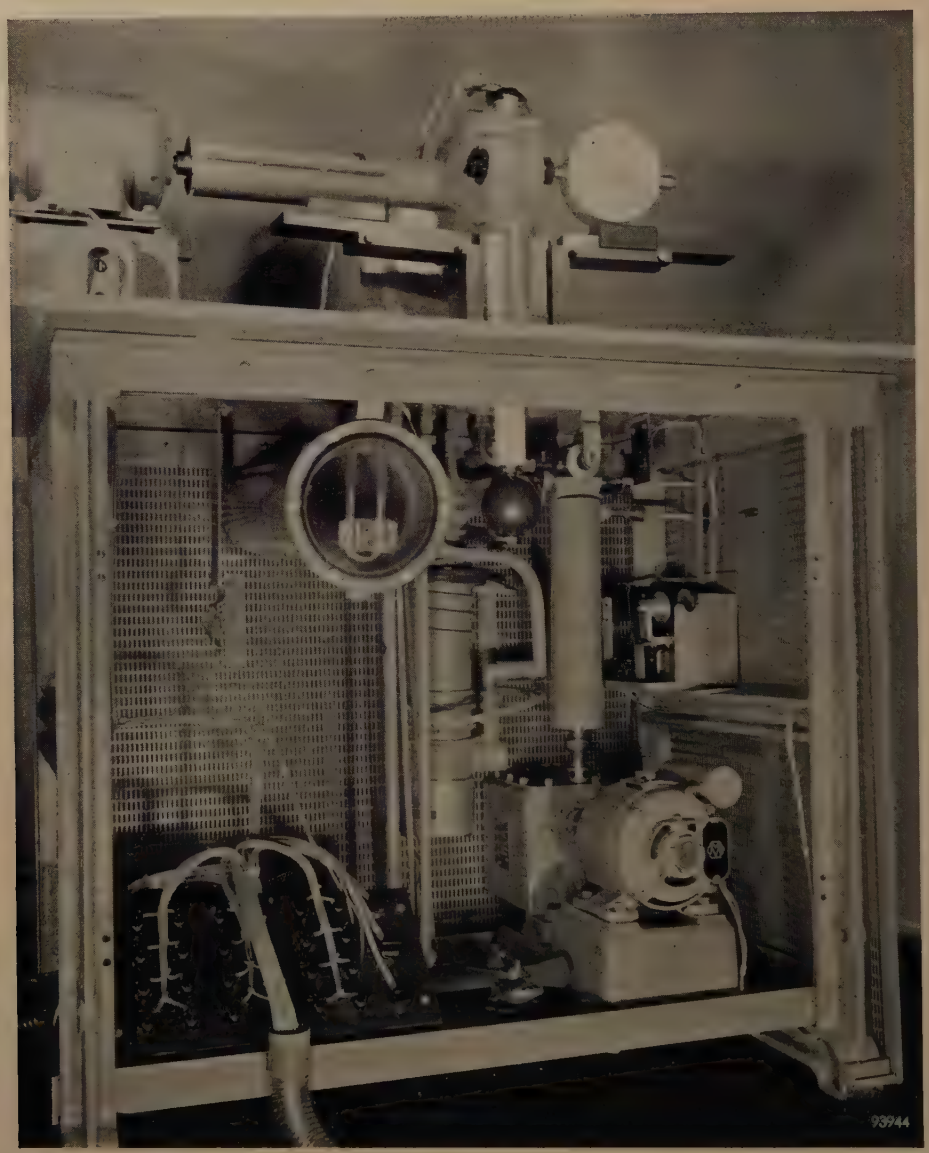

Fig. 4. The table on which the X-ray tube is mounted, and housing, underneath, the vacuum system and other auxiliaries. The rotary oil pump may be seen in the bottom right-hand corner (backing pressure 10^{-3} mm Hg). At the rear, in the middle, is the two-stage oil diffusion pump. It is possible with these pumps to obtain a vacuum of better than 10^{-5} mm Hg. Near the top of the compartment, centre, may be seen the lower end of the porcelain insulator which forms part of the cathode assembly. The metal sphere attached to the bottom of the insulator helps to dissipate heat; it is also the terminal for the high-tension cable (absent in this photograph). To the right of the insulator are the tube and magnet of a Penning manometer. The electrical part of this instrument is mounted half-way up the wall on the right. The large cylindrical container with end-window is the vacuum reservoir; inside it is a mercury manometer. The cable in the foreground goes to a separate control unit.

dissipate heat; the high-tension cable is attached to this sphere. Fig. 4 also shows the vacuum pumps and various other auxiliaries.

The voltage for the tube is derived from a three-phase high-tension transformer and six rectifiers. The transformer and rectifying valves are immersed in a water-cooled oil bath. The voltage for the transformer primary is derived from a variable three-phase transformer. This latter, and the oil tank just referred to, are separate from the main apparatus and are not visible in the photographs.

The control unit is mounted on a mobile rack. Also on this rack are three smoothing coils forming part of the high-tension circuit (a coil for each phase), and the stabilizer for the filament current. A cut-out, also mounted on the rack, switches off the high-tension supply should the anode current rise above a certain value.

The X-ray diffraction tube described here has now been in satisfactory operation for some years at the Laboratory of Crystal Chemistry of Utrecht University.

W. J. H. BEEKMAN, A. VERHOEFF and H. W. van der VOORN.

ANNEALING THE ENVELOPES OF TELEVISION PICTURE-TUBES

The envelope of a television picture-tube consists of three parts: the screen, "cone" and neck. When these parts are fused together, stresses are set up in the glass. To relieve these stresses, the envelopes are conveyed on a moving belt through a long annealing oven. The above photograph shows the process in operation in the new television tube factory in Eindhoven.

A METHOD OF SEALING THE WINDOW AND CONE OF TELEVISION PICTURE-TUBES

by A. H. EDENS.

666.1.037.4:621.385.832:621.397.62

This article gives some idea of the various problems which arise in the mechanized working of mass-produced heavy glass parts which do not possess rotational symmetry.

Thin-walled glass parts are generally sealed together by heating them with a number of gas jets which are aligned radially, as shown in *fig. 1a*. The hot edges are pressed together, producing a joint as illustrated in fig. 1*b*. By immediately stretching slightly the joined parts, and sometimes rolling the area of the seal, inside and outside, a joint is obtained which, as regards wall-thickness, differs little from the rest of the structure (fig. 1*c*). A case in which such a technique is employed, viz. the sealing of the window and cone of a special type of cathode-ray tube, was described about a year ago in this Review [1]).

At Eindhoven, the above-mentioned difficulty is avoided by using a method of sealing in which the edges to be sealed are heated "head-on", that is to say with gas jets head-on to the edges instead of radially directed jets. The geometry of the method is illustrated in *fig. 2*. We shall now briefly consider some of the special features of this method.

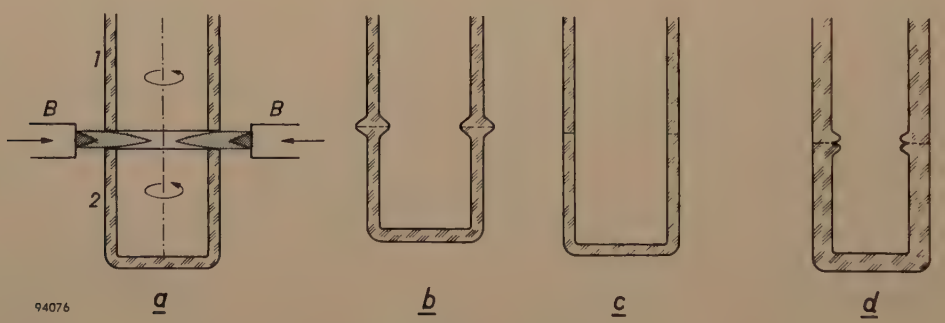

Fig. 1. *a*) For sealing two thin-walled sections *1* and *2* the sections are heated, while rotating, by burners *B*, the jets being directed radially on the glass parts to be joined.
b) Joint obtained by pressing the hot ends together.
c) Joint after stretching.
d) The sealing of two thick-walled sections by the same method does not produce a good joint (notch on the inside).

A satisfactory joint cannot be obtained, however, by using this same method for sealing together thick-walled parts, such as the window and cone of a glass television picture-tube (wall thickness 5 to 6 mm or more). In this case, sealing no longer takes place over the whole surface of the edges, since the edges during heating exhibit a radial temperature gradient (the direction of the gas jets). If the temperature on the outside of the bulb is correct, the temperature on the inside is too low, and consequently the surface tension cannot overcome the high viscosity of the glass at this point. This gives rise to an imperfect joint on the inside (fig. 1*d*). This is particularly undesirable if the joint is subsequently to be subjected to a heavy mechanical load, as it is in the case of an evacuated picture-tube.

During the sealing process the two glass parts are kept rotating, both in the conventional method with radial flames and in the head-on system. If the sections were not rotated, then, in spite of the distribution of the heat supply among many small

[1]) F. G. Blackler, Rectangular cathode-ray tubes of high aspect ratio, Philips tech. Rev. **18**, 298-300, 1956/57 (No. 10).

gas jets, each separate jet would inevitably cause local overheating, giving rise to drops of molten glass and possibly to gas bubbles. Moreover, rotation is desirable to compensate for minor differences

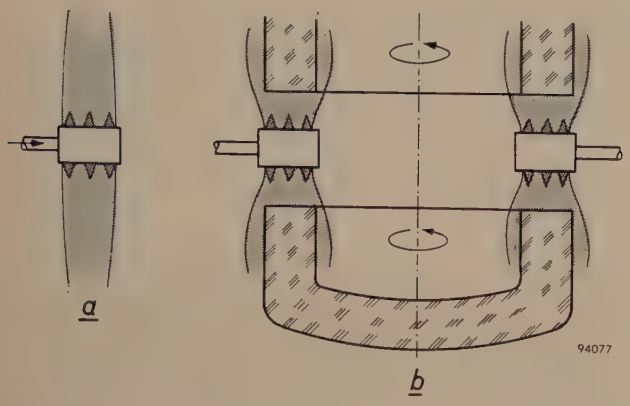

Fig. 2. By the method developed at Philips, thick-walled glass parts are sealed by means of burners (*a*) whose gas jets are directed head-on to the edges to be joined (*b*).

in the functioning of the usual gas-oxygen burners, caused by dirt or slight differences of adjustment: with rotation the heat from each burner is spread out over the entire surface.

For glass parts having rotational symmetry, no problems are entailed by rotation which, depending on the dimensions, takes place at a speed from 15 to 30 r.p.m. The burners are kept stationary with respect to the two synchronously rotating edges, resulting in a uniform relative movement of each gas jet over the whole area of the edge. With picture-tubes, however, the window and cone of which are substantially rectangular with rounded corners, special measures are called for in order to ensure that, during the rotation of the glass parts, each part of the edge receives an equal supply of heat.

In the first place the burners must be moved radially to and fro, so as to keep them always directed on the edges being heated. This requirement is also imposed in the conventional method of radial heating (see the article quoted under [1])). In the head-on method a further requirement is that the box-shaped burner heads, each of which contains a series of jets, above and below, should be swivelled during motion in such a way that the rows of jets are at each instant properly aligned between the edges of window and cone. This requirement is fulfilled with the aid of the mechanism illustrated in *fig. 3*. Each burner is fixed to a small carriage whose two rollers rest against the periphery of a flange which is profiled to the same form as the edges to be sealed. The carriage is pivoted on a block sliding in a radial guide, the block being kept pressed inwards by means of a piston actuated by compressed-air. In this way, then, the burners automatically move radially and swivel so as to maintain correct alignment on the edges. This is not enough, however. A glance at fig. 3 shows that during rotation the four corners of the parts to be sealed together are exposed to each burner longer than the centres of the sides. To ensure uniform heating a further measure is therefore necessary: the fuel feed to the burners must be varied in a specific manner during their movement.

Before we go on to discuss how this is done, we may complete the general description of the process of sealing glass parts by this method. Around the bulb twelve burners are disposed, uniformly positioned over an arc of 247.5° (angular separation 22.5°); see *fig. 4*. As soon as the two edges are heated to a sufficiently high temperature, i.e. after head-on heating for about 15 seconds, the burners are withdrawn from between the edges, and the window section of the picture-tube is pressed against the cone section by an upward movement of the window support. The butt joint thus obtained, and illus-

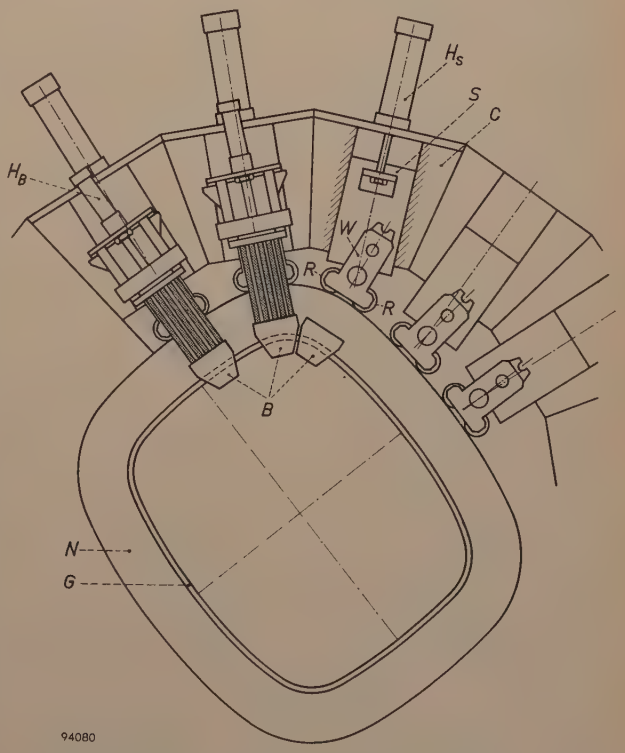

Fig. 3. Mechanism for guiding the burners in such a way that the rows of gas jets in head-on heating are always directed on the edges G of the substantially rectangular glass sections. Only two of the twelve burner systems are shown complete in the drawing. Each burner head B is mounted on a carriage W, which is pivoted on a block S and which, with two rollers R, is kept pressed against the profiled flange N by a compressed-air actuator H_S (C is a guide for the block S). Each burner can be moved forward (for head-on heating) by a small compressed-air actuator H_B, mounted on the carriage, and drawn back for after-heating.

trated in fig. 1*b*, is stretched by a subsequent lowering of the window support by a few millimetres: the joint then stretches by virtue of the weight of the window. In order to prevent the temperature of the joint from dropping too much during the time needed for the stretching (or "sagging") process, after-heating is applied by means of radially directed gas jets. The manner of stretching can be controlled by applying the after-heating higher or lower in the area of the seal, and in this way joints of good uniformity in wall thickness can be obtained.

The after-heating, during which the bulb continues to rotate, is effected with the same burner heads by flames from rows of jets in the front face of the heads; see *fig. 5a* and *b*). These jets and their fuel feed constitute an entirely separate system. When the burners are withdrawn from between the edges, the fuel feed is automatically switched over from the system for head-on heating to the system for after-heating. The withdrawal of the burners is brought about by separate compressed-air actuators which move the burners with respect to the swivel-

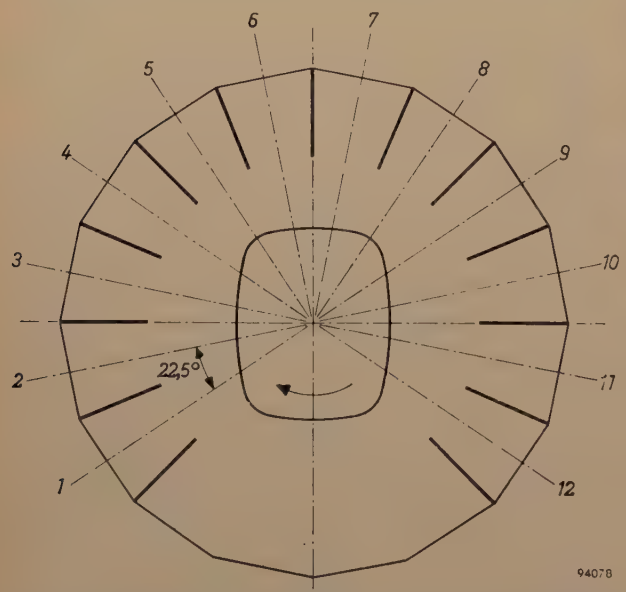

Fig. 4. Arrangement of the burners *1* to *12* around the glass parts to be sealed. The workpieces are accessible from the front.

ling, rollered carriages, the rollers always remaining pressed against the profiled flange. Thus the burners continue their radial and swivelling motions during the after-heating of the rotating bulb. For after-heating, the same periodic regulation of the fuel feed is necessary as for head-on heating.

The periodic variation required for the fuel feed can be derived from *fig. 6a*. In this figure, which refers to a 17″ picture-tube, the relative speed of

a

b

Fig. 5. The burner head, (*a*) with the jets for head-on heating in operation and (*b*) with the jets for after-heating in operation.

a burner with respect to the glass passing under it is plotted against time, or rather — which amounts to the same thing — against the angular position α of the radius vector of the carriage (fig. 6*b*). Without the swivelling of the burner the result would be the smaller variation indicated by the dashed curve in fig. 6*a*; each maximum of this curve corresponds to the passing of one corner of the window, where the linear speed of the glass is, of course, greatest. However, since the swivelling of the burner carriage, which at that point is opposed to the linear motion of the glass, is also fastest at the corners, a deep minimum is in fact produced at this point in the relative speed of the glass with respect to the burners; see the fully-drawn curve. It can be seen from the figure that the relative speed during the rotation of the glass varies by about a factor of 2.

Since slight temperature differences along the edges to be joined can be tolerated, it is not necessary that the variation of the fuel feed should follow accurately the form of the curve in fig. 6*a*. In practice a periodic variation between two levels is found to be sufficient (except for a small modification to be mentioned later). This variation is carried out in the following way.

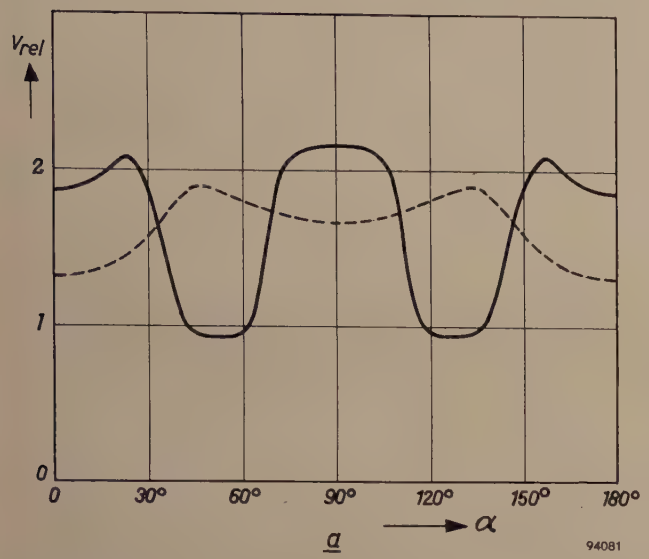

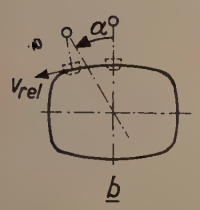

Fig. 6. *a*) Relative speed (v_{rel}) of a burner with respect to the glass, as a function of the position (angle α) of the burner carriage with respect to the revolving glass parts. The broken curve is that which would be obtained if the burner, instead of swivelling, were always pointed radially inward. *b*) Sketch illustrating the definition of α.

The two systems (for head-on and after-heating) in each burner are each fed via a separate ejector device to which oxygen is supplied under pressure and which sucks in gas. Ejector-fed burners of this kind generally operate on an excess of gas, as they do in our case. The primary flame, the familiar blue cone, forms directly over the holes of the burner; the amount of gas burnt here corresponds to the quantity of oxygen in the gas-oxygen mixture. The excess gas burns on the air in the atmosphere. Since each burner head with its jets moves at a distance of only about 7 mm from the edges of the glass parts, the quantity of heat delivered at any instant to these edges is mainly determined by the flow of oxygen at that moment from the burner. The burner is therefore regulated by varying the pressure of the oxygen fed to the ejector. The regulating device is represented in *fig.* 7. The oxygen flows through the device via two openings, a wide one which can be closed by a valve, and a much narrower one (a constriction). The valve is actuated by a cam which releases the valve stem (this being under spring pressure), thereby closing the valve whenever one of the four corners of the glass parts approaches the particular burner. The oxygen can then flow only through the constriction, over which an appreciable pressure drop exists; the open valve, on the other hand, causes almost no pressure drop. The oxygen pressure at the ejector inlet thus varies periodically between a low value (at the corners) and a high one.

We shall now mention some details of the actual mechanism. The regulator illustrated in fig. 7 supplies oxygen to the ejectors of two diametrically opposite burners — for example No. 1 and No. 9 in fig. 4 — since two oppositely situated burners must receive the same oxygen sypply at each instant. The four burners Nos. 5 to 8, which have no opposite numbers, each have a regulator of their own. For head-on heating there are therefore eight regulators, which are incorporated in a single block and whose valves are actuated with appropriate phase differences by eight cams mounted on one rotating shaft. This camshaft must of course have a certain fixed angular adjustment with respect to the profiled flange around which the burners move (and hence with respect to the revolving glass).

For the after-heating systems the regulation is carried out in an identical manner; here too there

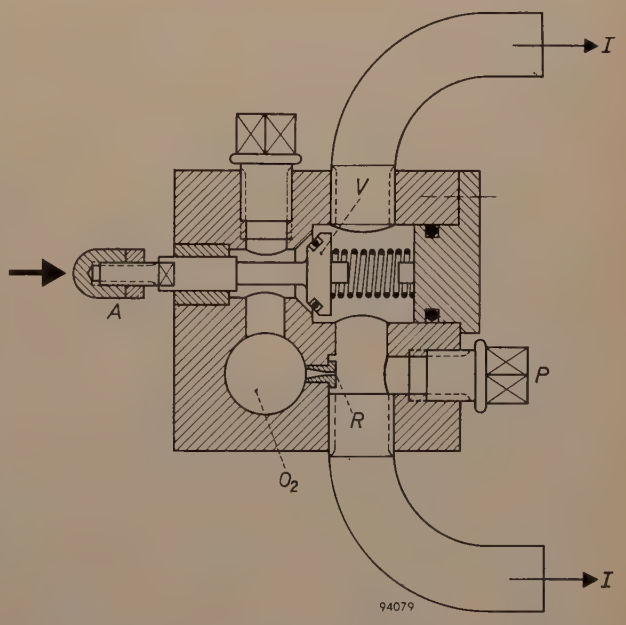

Fig. 7. Regulator for periodically varying the pressure under which the oxygen is fed to the ejector *I* of a burner. (This regulator serves two ejectors.) O_2 oxygen feed to regulator; *V* valve, which is opened by the action of a cam on the stem (adjustable with nut *A*) against spring pressure; *R* constriction, the only route which the oxygen can take when *V* is closed, resulting in a reduced pressure in the pipe to the ejector(s).

are four double and four single regulators. These are incorporated in a second block, in the same order as the regulators for head-on heating, so that they can be operated by the same cams. The two series of regulators differ only in the size of the constrictions, since the burner jets for head-on heating pass a greater quantity of fuel mixture than those for after-heating. The constrictions in the regulators with a double ejector connection are, of course, also wider than those with a single connection. The size of the constrictions is chosen according to the bulb under production (that is to say, to the curve in fig. 6*a*). For the production of other bulbs, larger picture-tubes for example, the constriction in each regulator can be changed after first removing the plug P in fig. 7. It is also necessary, as a rule, to change the cams.

In one full revolution of the glass each cam must complete two identical cycles. For simplicity, therefore, the cams have only two flats instead of four (for the four corners), and the cams perform two revolutions for each revolution of the glass workpiece. With a view to convenience of installation and easy access to the supply pipes, the two blocks containing the regulators for head-on and after-heating (K' and K'' respectively, *fig. 8*) are mounted directly facing each other at opposite sides of the cams. This entails that regulators K' and K'', which are actuated by the same cam, must operate on burners which are mounted in the machine at an angular separation of 90°. Thus the cam which actuates regulator $K'_{1,9}$ is also responsible for K''_5, the cam for $K'_{2,10}$ also relates to K''_6, and so on. In this way, in after-heating as well as in head-on heating, all burners are automatically controlled in the correct phase with respect to the revolving glass parts.

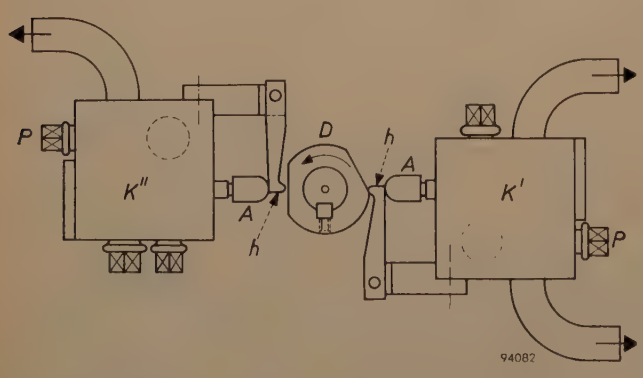

Fig. 8. The block containing eight adjacent regulators K' for head-on heating, and a similar block with regulators K'' for after-heating, are both driven by a single camshaft with eight cams D. The end A of each valve stem is not directly in contact with its associated cam, but rests against a separate rocker arm h, so that the valve stem is subjected only to an axial load.

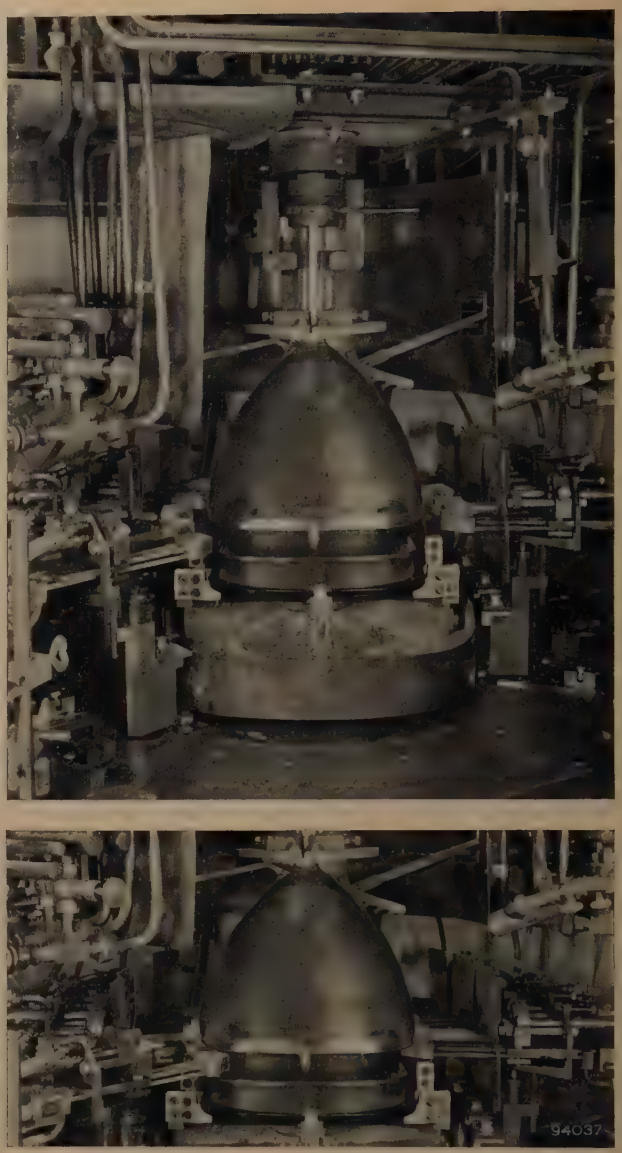

Fig. 9. *a*) View of the glass-sealing machine, showing the window and cone sections of a 17″ picture-tube in position. The burners are withdrawn.
b) Burners moved forward between the edges to be sealed (in the actual process the burners are not moved into position until the glass has first been pre-heated for a certain period; to avoid photographic complications, the pre-heating stage was omitted in taking these pictures).

In the set-up as described, all twelve burners pass through the same control cycle. In principle this is not necessary, since at each point of the edge the glass will experience the average effect of all burners. In fact, in the case of one pair of burners for head-on heating, a modification is made to the cycle described: the cam in this case is provided with an additional flat such that the burners in question (and the after-heating burner served by the same cam) receive less fuel in the middle of the long side of the window and cone. Before this modification was applied a hot spot in the glass was found corresponding to the trough at $\alpha = 0°$ in the curve in fig. 6*a*.

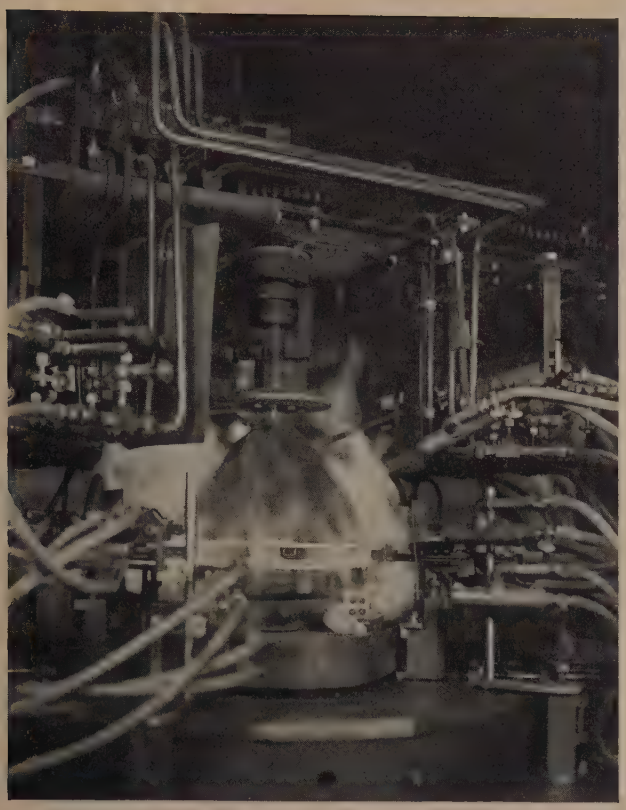

a

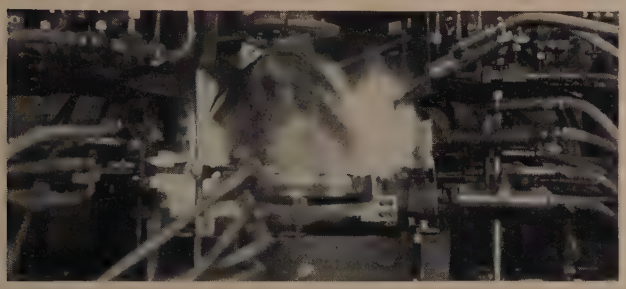

b

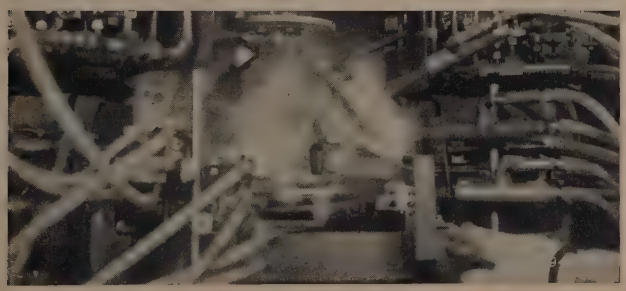

c

Fig. 10. A tube of the type shown in fig. 9 in the process of being sealed:
a) The edges to be joined are heated to the required temperature.
b) The edges have been pressed together and after-heating has begun, while the joint is allowed to stretch.
c) Rolling of the joint after stretching.

Finally, we give a number of photographs of the glass-sealing machine, which illustrate the manufacture of a 17″ picture-tube. To facilitate the handling of the large glass components, both before and after sealing, the machine is constructed such that the picture-tube is mounted in it with its axis vertical. *Fig. 9a* shows the window and cone section mounted in position and with the burners withdrawn; in fig. 9*b* the burners are seen in the sealing position, the burner heads being between the edges of window and cone.

After the sections have been set in rotation and preheated, the head-on heating begins; this lasts, as stated earlier, about 15 seconds, during which time the glass completes about four revolutions. In *fig. 10a*, head-on heating has just been completed and the burners are again in the withdrawn position. The edges of window and cone are pressed together, after-heating of the sealed zone begins (fig. 10*b*) and the window support drops slightly to stretch the joint. One detail worth mentioning is that at the moment the gap between window and cone is sealed, a slight, adjustable over-pressure is created inside the bulb. This serves to compensate for the pressure exerted by the gas jets on the area of the seal during after-heating, and which might otherwise cause this area to collapse. After the joint has been stretched, it is smoothed on the outside with a graphite roller (fig. 10*c*).

Most of the operations described are performed automatically, being programmed by means of a camshaft at the rear of the machine.

Summary. For sealing thick-walled glass parts, such as the window and cone of a picture-tube, a method is used at Philips in which the glass parts, while rotating, are heated by gas-oxygen jets directed head-on to the edges to be sealed. Twelve burner heads are placed between the edges of the roughly rectangular workpieces, which are in rotation; by means of a guide mechanism the heads are simultaneously moved radially and swivelled in such a way that the rows of burner jets are always directed on the edges of the workpieces. To compensate for the periodic variations in the speed of each burner relative to the glass, the fuel feed (oxygen pressure) of each burner is varied periodically in the correct phase. This also applies to the after-heating of the seal by the same burner heads.

FABRICATION OF SAPPHIRE AND DIAMOND STYLI FOR GRAMOPHONE PICK-UPS

681.84.081.32

Gramophone pick-ups with sapphire and diamond styli have largely replaced the older pick-ups which used interchangeable steel needles. One important reason for this lies in the enormously lower wear suffered by these hard materials. Although they are very much harder, sapphire and diamond cause much less record wear than steel needles: it is found that both distortion of reproduction and record wear are more dependent on the *shape* of the needle point than on other factors, so that the longer this is maintained the better. The photographs of *fig. 1* show how well sapphire and diamond needles maintain their shape, even after hundreds of hours of use. A steel needle wears to the groove shape after only one playing. Another important advantage of the sapphire and diamond styli is that the moving system of the pick-up can be made with a much smaller moment of inertia than in the older types with their comparatively massive steel needle and holder. In modern pick-ups using sapphire and diamond styli, the effective mass at the needle point may be as little as 3 mg, resulting in a cut-off frequency due to stylus/groove resonance of the order of 20 kc/s, which is well above the limit of the audible frequency range [1]).

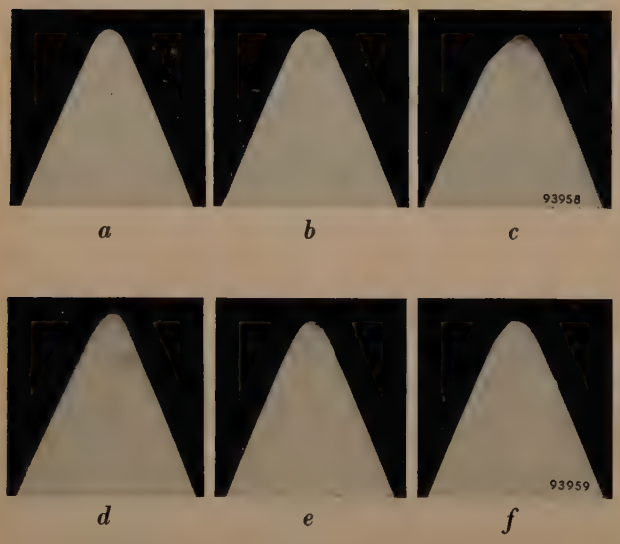

Fig. 1. Comparative shadow photographs showing the wear of a microgroove sapphire stylus and a microgroove diamond stylus (tip radius 25 μ). The vertical force on the needle amounted to 12 gram. For each stylus a new long-playing vinylite record was taken and the test continued throughout with the *same* record. It should be stressed that under these conditions the wear on the needle is far higher than ever occurs in practice. The microscopic particles worn from the needle are in normal circumstances distributed over a whole collection of records; here they are concentrated in the grooves of a single record, resulting in a much higher rate of wear. Furthermore, the photographs give no quantitative indication of the advantage of the diamond over the sapphire; in fact, the diamond may have a life of more than twenty times that of a sapphire point. *a*) Unused sapphire stylus. *b*) Sapphire, after 75 hours. *c*) Sapphire, after 175 hours. *d*) Unused diamond stylus. *e*) Diamond, after 150 hours. *f*) Diamond, after 300 hours.

Sapphire and diamond styli for gramophone pick-ups are manufactured in the Philips diamond-die factory at Valkenswaard (near Eindhoven).

Sapphire cylinders 3 mm long and 0.4 mm in diameter, cut from sheets of synthetic sapphire, are mounted in small rotating heads by means of shellac. A number of such heads are placed at an angle ($22\frac{1}{2}°$) to an equal number of cast-iron grinding wheels, the pores of which contain a little diamond dust in oil. The heads and the grinding wheels are rotated at high speed while at the same time the grinding wheels are given a slow reciprocating movement parallel to their surface in order to obtain uniform grinding (*fig. 2*).

In this way the cylinder is given a conical end. The process is stopped, however, before the cone is sharp-pointed, as this tends to cause breakages during further handling. The sapphire cylinder is then reversed and the coning operation repeated on the other end. Subsequently the needles are broken in half, ground to a length of 1 mm and cleaned, and are then ready for the radiusing of the points. This is done by placing a large number of them (several thousands) together in a bottle containing diamond dust in oil. The bottle is then vibrated for several days, after which the points are found to be spherical in shape. The radius becomes greater as the vibration is continued. In this way the required radius (25 μ for microgroove records, 75 μ for normal 78 r.p.m. records) is easily obtained [2]).

For diamond styli, selected stones are first cut parallel to the (111) plane to give plates 1.6 mm in thickness (*fig. 3*). From these plates cylinders 0.3 mm in diameter are cut by means of thin-walled nickel tubes rotating at about 10 000 r.p.m. and containing diamond dust in oil. The ends of the cylinders which will become the points of the styli are therefore in the (111) plane. This plane is chosen partly because of its great wear resistance [3]) but

[1]) For an explanation of these terms and a fuller discussion of the questions involved, see J. B. S. M. Kerstens, Mechanical phenomena in gramophone pick-ups at high audio frequencies, Philips tech. Rev. **18**, 89-97, 1956/57; also N. Wittenberg, A magnetodynamic gramophone pick-up, Philips tech. Rev. **18**, 101-109 and 173-178, 1956/57.

[2]) The same technique is used for rounding off the edges of quartz oscillator crystals.

[3]) See, for example, L. Schultink, H. L. Spier and A. J. van der Wagt, Philips tech. Rev. **16**, 91-97, 1954/55.

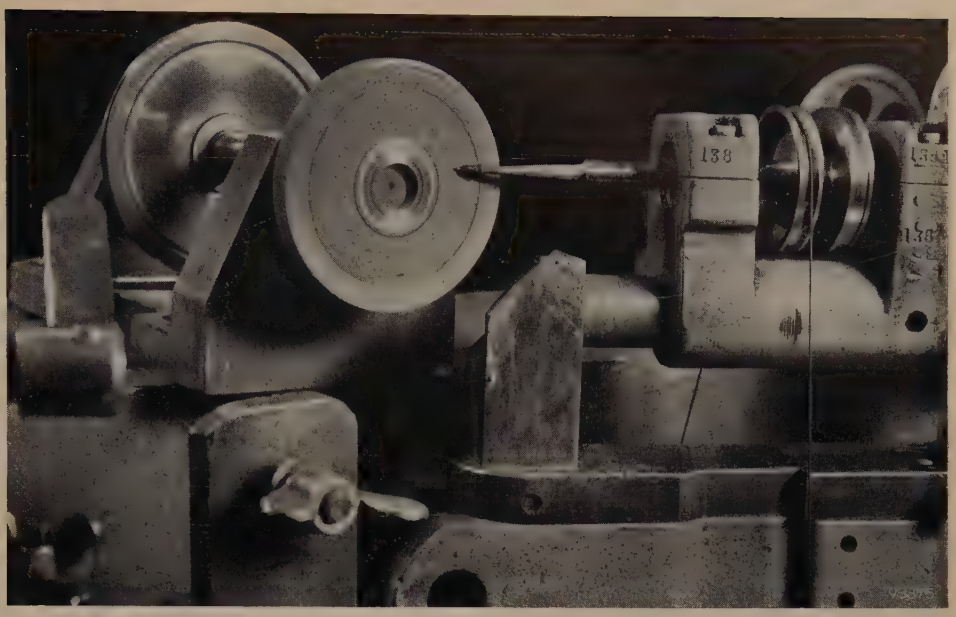

Fig. 2. Part of the 10-head machine for grinding cones on the ends of sapphire and diamond cylinders. The frame of the machine is suspended on four flexible steel strips. At one end of the machine a cam imparts a slow reciprocating movement to the whole frame, parallel to the surfaces of the grinding wheels. The sapphire or diamond cylinders are fixed in the rotating heads by means of shellac.

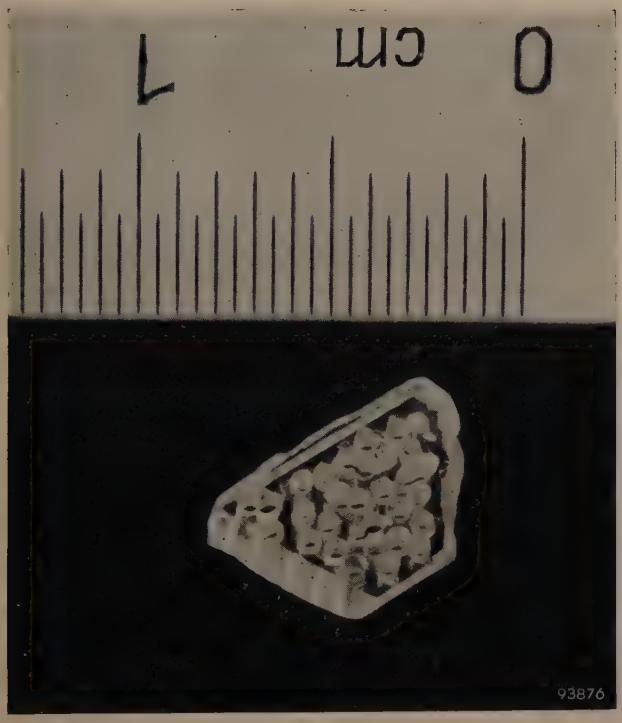

Fig. 3. Diamond platelet, 1.6 mm thick, cut parallel to the octahedral (111) plane and drilled out to give cylinders of 0.3 mm diameter (see fig. 4, above).

also because (111) faces of reasonable area can be cut from the natural crystal without too much loss of material. Next a cone is cut at each end of the cylinder in the same way as for sapphire. In the case of diamond, however, the operation takes about 10 times longer. The radiusing of the ends cannot be effectively performed by the technique used for sapphire in view of the greater hardness and the fact that the mass of the diamond styli is considerably less. Diamond styli are therefore radiused by hand on a special grinding wheel. The rotating head containing the diamond stylus is removed from the coning machine and set in the radiusing machine; the latter is equipped with a microscope for control of the operation. The radiusing takes about one minute. The diamond cylinder is then reversed in the rotating head and replaced in the coning machine; this is again followed by the radiusing operation. After cleaving the pointed cylinder in half and cleaning, the styli are ready for mounting. *Fig. 4* gives an idea of the size of the diamond cylinder and the finished stylus.

Of the original diamond, less than half can be drilled out into cylinders of the required dimensions. The remaining drilled stones are crushed to form diamond dust. Diamond dust is also recovered from

Fig. 4. Above, shadow photograph of diamond cylinder as bored from diamond platelet; below, shadow photograph of a finished stylus, 0.3 mm diam., 0.6 mm long.

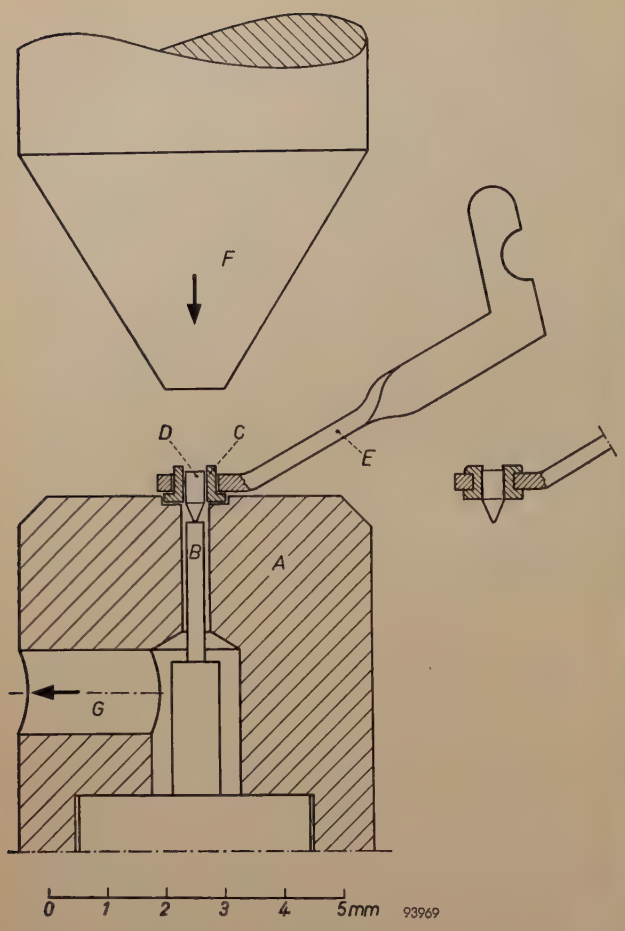

Fig. 5. Sketch of cleating jig (about 8× actual size). *A* vacuum jig, *B* stop, *C* aluminium bush, *D* stylus, *E* stylus arm, *F* punch, *G* vacuum line.

the vicinity of the various grinding operations by means of carefully placed shields. After cleaning and grading into size ranges by centrifuging, the dust can be used again. There is, however, a surplus (mainly of the finest grades) and this is used for other purposes, e.g. for polishing in metallography.

Both the sapphire and the diamond styli are mounted on the stylus arm by the same technique.

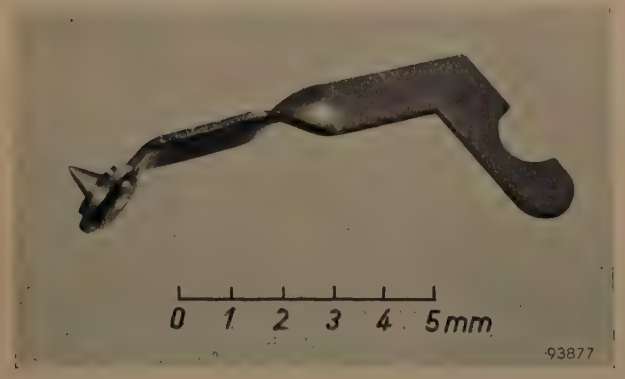

Fig. 6. Finished stylus mounted on stylus arm.

A tiny aluminium bushing is picked up on the end of a 0.3 mm bore nickel tube through which air is sucked (tweezers are not very suitable for handling such small objects). The bushing is placed on a hollow jig mounted in a light press (*fig. 5*). Air is also sucked through this jig and the dimensions and pressure are so chosen that the bushing is taken over from the nickel tube and seated in the correct position. A stylus is then placed inside the bushing, point downwards; the suction causes the point to come up against a stop which ensures a constant projection of the stylus below the stylus arm. The latter is placed round the bushing and the press operated, providing a completely rigid mounting for the stylus (*fig. 6*).

Fig. 7. Projection microscope (magnification 50×) for the individual inspection of mounted sapphire and diamond styli. The three lines on the screen serve for the checking of dimensions and alignment.

The mounted styli are then individually checked in low-power projection microscopes (*fig. 7*).

A. W. PLOEGSMA.

ABSTRACTS OF RECENT SCIENTIFIC PUBLICATIONS BY THE STAFF OF N.V. PHILIPS' GLOEILAMPENFABRIEKEN

Reprints of these papers not marked with an asterisk * can be obtained free of charge upon application to the Philips Research Laboratory, Eindhoven, Netherlands.

2512*: J. Volger and J. M. Stevels: Continuation des recherches expérimentales sur les pertes diélectriques de certains verres aux basses températures (Verres et Réfractaires **11**, 137-146, 1957, No. 3).

Translation of article in Philips Res. Repts **11**, 452-470, 1956 (see these Abstracts No. **R 301**).

2513: J. H. Uhlenbroek and M. J. Koopmans: Investigations on agricultural fungicides, II. Compounds structurally related to trichloromethyl thiolsulphonates (Rec. Trav. chim. Pays-Bas **76**, 657-665, 1957, No. 7).

The preparation and the fungitoxic properties of some thiolsulphonic esters (type p-$CH_3C_6H_4SO_2SR'$) and of some reaction products of trichloromethanesulphenyl chloride with thiosulphonic acid salts and with thiophenols are described in this paper.

2514: J. H. Uhlenbroek and M. J. Koopmans: Investigations on agricultural fungicides, III. The reaction between trichloromethanesulphenyl chloride and benzoic acid (Rec. Trav. chim. Pays-Bas **76**, 666-668, 1957, No. 7).

A mixed anhydride of trichloromethanesulphenic acid and benzoic acid has been prepared for which the name of benzoic trichloromethanesulphenic anhydride is proposed. Some chemical and biological properties of the new compound are described.

2515*: K. Compaan and Y. Haven: La diffusion de radiotraceurs dans les solides;
J. L. Meijering: Diffusion des atomes en insertion;
A. van Wieringen: Etude du passage non-stationnaire de l'hélium à travers le silicium et le germanium à l'aide d'un spectromètre de masse
(La diffusion dans les métaux, edited by J. D. Fast, H. G. van Bueren and J. Philibert, Philips Technical Library, 1957).

See book notice below, p. 332.

2516: S. Duinker: L'application des ferrites à la modulation dans divers domaines de fréquence (Atti del Congresso Scientifico, sezione elettronica, July 1956, pp. 571-585).

Survey of ferrite applications for modulation in tuned circuits, in phase and frequency modulators, in magnetic modulators and in absorption modulators for S.H.F.

2517: E. G. Dorgelo: Some technological aspects of U.H.F. triode design (Le Vide **12**, No. 67, 3-8, 1957).

It is well known that the efficiency of a triode decreases at higher frequencies. This is due to the fact that the transit time of the electrons is no longer negligible in comparison with the period of the oscillations. The transit time can be made small by mounting the electrodes very close together and by applying large potential differences. Both measures, however, give rise to large current densities. As a result, the design of high-frequency transmitting valves comes against a number of technological problems, of which two are mentioned in this article: cathodes with a high current-density emission and grids with a large specific dissipation. A new material for the grids (K-material) is described for which continuous dissipations of up to 30 W per cm^2 are possible. The high-frequency resistance is sufficiently low to permit use in transmitting valves for decimetre waves. The article concludes with a short description of such a valve.

2518: E. G. Dorgelo: Gitterprobleme bei Sendetrioden in Schaltungen der industriellen Elektronik (Funk-Technik **12**, 528, 530 and 532, 1957, No. 15). (Grid problems in transmitting triodes used in industrial electronics; in German.)

It is common practice to include in the published data of transmitting valves, so-called limiting values for grid input. As long as this value is not exceeded, there ought to be no excessive thermal emission from the grid. There are three contributions to the total power, dissipated in the grid: heat generated by electron bombardment, absorbed radiation from other electrodes and R.F. losses. In general, the user can measure only the first mentioned. Even here errors can be made due to the fact that the measured grid current is not representative of the number of electrons arriving at the grid. When secondary emission is present, other electrons will leave the grid and the measured current smaller than the actual grid current. In view of t

fact that the valve manufacturer usually does not give an indication what he actually means by the published value and also because it is physically impossible to measure the true grid currents, it is rather difficult for the user to evaluate the quality of a valve merely from the published data. In an example the author compares two equivalent valve types of different make. Measurements reveal that the valve with the best-looking published data shows the highest thermal emission of the grid.

2519: H. P. J. Wijn, H. van der Heide and J. F. Fast: Ordering in cobalt-ferrous ferrites (Proc. Instn. Electr. Engrs. **104 B**, suppl. No. 7, 412-417, 1957).

Various cobalt-ferrous ferrites show a constricted hysteresis loop. After magnetic annealing of the samples, the loop becomes rectangular. It appears that the magnetic annealing creates in each crystal a uniaxial anisotropy in a direction which is not necessarily the direction of the applied magnetic field but a crystallographic direction nearest to it. It is suggested that directional ordering is the most probable origin of the anisotropy found.

2520: E. W. Gorter and C. J. Esveldt: Square-loop ferrites obtained by magnetic annealing of new compositions (Proc. Instn. Electr. Engrs. **104 B**, suppl. No. 7, 418-421, 1957).

Extension of the work abstracted in No. **2519** to cobalt ferrites of other composition. When a ferrite containing cobalt is cooled in a magnetic field, diffusion of Co^{2+} ions causes a uniaxial anisotropy that is apparent in a rectangular hysteresis loop. In various ferrites containing only a small proportion of Co^{2+} ions, this diffusion is very slow. For the composition $(Mg_{0.6}Ni_{0.4})_{0.98}Co_{0.02}Fe_2O_4$, however, this diffusion is fast; on cooling in a magnetic field, a weak coercive force and an extremely rectangular hysteresis loop are obtained. The loop is practically independent of temperature.

2521: H. P. J. Wijn and H. van der Heide: Pulse-response properties of rectangular-loop ferrites (Proc. Instn. Electr. Engrs. **104 B**, suppl. No. 7, 422-427, 1957).

An analysis of the voltage pulses obtained across a secondary winding of a ferrite core on reversing the magnetization shows that in the reversal two stages should be distinguished, namely a fast response, related to a magnetization by rotations, and a slower response due to the displacements of domain walls. The viscous movement of the domain walls determines the switching time of the core. It appears that the switching times of rectangular-loop ferrites with widely varying chemical compositions are always of the order of magnitude of one microsecond when the coercive force is of the order of magnitude of one oersted. Higher values of the coercive force mostly go hand in hand with an increased switching time. In order to obtain some information about the origin of the damping of domain-wall displacements, switching times have been measured as a function of temperature and as a function of a uniaxial pressure applied to the core. In the temperature range —115 to +250 °C the switching time of an arbitrarily chosen rectangular-loop ferrite did not decrease more than by a factor of about three. A uniaxial pressure applied to a ferrite also increases both its coercive force and its switching time. It appears that the switching time is greater when the anisotropies in the ferrite are greater. This can at least partly be explained by the increased distance between the walls in the case of higher magnetic anisotropies.

2522: C. M. van der Burgt: Ferrites for magnetic and piezomagnetic filter elements with temperature-independent permeability and elasticity (Proc. Instn. Electr. Engrs. **104 B**, suppl. No. 7, 550-557, 1957).

In recent experiments the compositions and methods of preparation of various ferrites were varied with the aim of achieving optimum magnetic, magnetomechanical and mechanical performance. Essential improvements of the temperature dependence of the permeability, the piezomagnetic coupling coefficient and the mechanical resonant frequencies have been obtained. These were achieved by small cobalt substitutions in nickel and lithium ferrite and in mixed nickel-zinc and lithium-zinc ferrites. The total variations of the mechanical resonant and anti-resonant frequencies of ferrite filter elements in the temperature range 20-50 °C are normally 0.10-0.25% in existing commercial nickel and nickel-zinc ferrites, but have been reduced to 0.03% or less. The coupling coefficient at remanence of such a stable ferrite may be well above 0.20 with a suitably modified sintering treatment. Since the mechanical Q-factors are usually much better than 2000, such ferrite vibrators can be profitably applied to the construction of electrical and electromechanical band-pass filters. The cobalt substitutions, apart from leading to a very low temperature coefficient of the real part of the permeability, also decrease the imaginary part, so that these cobalt-substituted ferrites have a high figure of merit. (See also Philips tech. Rev. **18**, 285-298, 1956/57 (No. 10), and No. **R 310** of these Abstracts.)

2523: E. W. Gorter: Chemistry and magnetic properties of some ferrimagnetic oxides like those occurring in nature (Adv. Phys. **6**, 336-361, 1957; No. 23).

This review paper, given for the Conference on Rock Magnetism (London, November 1956), mainly deals with previous work on ferrimagnetic oxides with spinel structure, described in Nos. **R 248, R 249** and **R 253** of these Abstracts, inasfar as it has a bearing on the ferrimagnetic oxides occurring in nature. In § 1 a more suitable representation of the composition diagram FeO-Fe_2O_3-TiO_2 is proposed. § 2 treats the cation distribution among tetrahedral and octahedral lattice sites and its methods of measurement, the valency of the transition ions present and the saturation magnetization as depending on composition, and discusses the difficulty of establishing the presence of miscibility gaps in a solid-solution series. § 3 discusses the relative orientation of the ionic magnetic moments in the spinel, hematite and pseudobrookite structures, as derived from Anderson's theory. It is shown that none of the explanations so far given for the behaviour of ilmenite, $FeTiO_3$, are satisfactory. In § 4 attention is drawn to the probability of exchange coupling between two phases as a governing mechanism for reverse thermoremanent magnetization.

2524: J. L. Meijering: Diffusion du fluor dans l'argent solide (Rev. Métallurgie **54**, 520-522, 1957, No. 7).

By heating silver containing e.g. 0.05% Mg in molten AgF, two diffusion zones are obtained. The two sharp boundaries are not affected perceptibly by grain boundaries. This "internal fluorination" causes hardening. Probably the inner zone contains MgF_2 and the outer zone a double fluoride like $AgMgF_3$.

2525: F. C. de Ronde: Un élément simple pour mesurer des impédances en ondes centimétriques et millimétriques: La terminaison variable à réglages indépendants et à lecture directe du module et de l'argument du coefficient de réflexion (Arch. des Sci. **10**, fasc. spéc. 6e Colloque Ampère, Rennes-St.-Malo, April 1957, pp. 66-67).

Brief note on a calibrated, direct-reading microwave impedance. An absorbing vane is fixed on a plunger which can be moved axially and also rotated over 90° in a circular waveguide. The modulus of the reflection coefficient depends on the angular position of the plunger and its argument on the axial position.

2526: F. C. de Ronde: Une nouvelle méthode de mesure de la constante diélectrique et de la perméabilité magnétique des matières solides en ondes centimétriques (Arch. des Sci. **10**, fasc. spéc. 6e Colloque Ampère, Rennes-St.-Malo, April 1957, pp. 68-70).

Brief description of a new method for measuring dielectric constant and magnetic permeability in solids at microwave frequencies. The method involves direct measurement of the characteristic impedance of a waveguide filled with the material.

2527: K. Rodenhuis: A 4000 Mc/s triode with L-cathode construction and circuit (Le Vide **12**, No. 67, 23-31, 1957).

Two valves, the EC 56 and the EC 57, for use in beam transmitters are described in this article. The use of L-cathodes, which give long life even at high current densities, and of discs of high H.F. conductivity, leads to an efficiency and a gain which are relatively high for triodes. Some details of the design and of the method of manufacture are given. The behaviour of the valves in an amplifier is discussed. The input impedance is given particular attention. The feedback is found to depend closely on the amplification factor of the valve and to exert an influence on the output power attainable. Finally various other applications of the valves are mentioned. (See also Philips tech. Rev. **18**, 317-324, 1956/57 (No. 11) and **19**, 145-156, 1957/58 (No. 5).)

2528: J. Verweel: The space-charge distribution in a static magnetron (Le Vide **12**, No. 67, 32-42, 1957).

In a non-oscillating cut-off magnetron the motion of the electrons gives rise to a space-charge cloud round the cathode. It is shown that by means of a narrow electron beam, injected parallel to the cathode, the electron paths can be imaged on a fluorescent screen. The electrons are found to describe cycloidal paths starting from the cathode; the radial velocity can be derived from the tangential component of the (thermal) initial velocity. The paths of the electrons are found to be strongly dependent on their initial velocity. To a first approximation, the density of the space-charge cloud is constant.

2529: A. Versnel: Magnetless magnetron (Le Vide **12**, No. 67, 59-63, 1957).

An oscillator tube is described which shows some resemblance to a magnetron both in construction and in operation. It differs from a magnetron, however, in that the path of the electron beam is

determined electrostatically. The beam moves in circular paths between two concentric cylinders. The inner cylinder, which is at a higher potential than the outer one, forms part of an H.F. circuit. In this respect also it differs from a magnetron, where the outer cylinder forms part of the resonant circuit. The maximum beam current and the oscillator frequency are calculated as functions of the electron velocity, and the results are compared with experimental observations. It is amusing to notice that the electrons behave as the electric analogue of planetary satellites: the orbiting electrons are in equilibrium with the attractive force of the electrostatic field.

2530: J. J. Balder: Illuminated borders to picture screens (Light and Lighting **50**, 245-250, 1957, No. 8).

A series of tests was carried out in which a person looking at a picture screen was asked to give his opinion as to the ideal luminance and width of a uniformly illuminated border round the picture giving optimum viewing comfort. The observations were made by 20-25 persons for a number of luminance levels of both screen an surroundings. (See also Philips tech. Rev. **19**, 156-158, 1957/58 (No. 5).)

2531: P. Westerhof and J. A. Keverling Buisman: Investigations on sterols, IX. Dihydroderivatives of ergocalciferol (Rec. Trav. chim. Pays-Bas **76**, 679-688, 1957, No. 8).

Some partially hydrogenated derivatives of ergocalciferol are described; their structures are discussed, and their activities in raising the serum calcium level of rats are reported.

2532: F. J. Mulder, J. R. Roborgh, Th. J. de Man, K. J. Keuning and K. H. Hanewald: A chemical routine determination of vitamin D; correlation with the biological determination (Analysis of fat soluble vitamins II) (Rec. Trav. chim. Pays-Bas **76**, 733-746, 1957, No. 8).

A chemical routine method for the determination of vitamins D_2 and D_3 in a number of preparations is presented. The results obtained agree very well with those obtained with the rat and chick assays respectively.

2533: K. J. Keuning, G. J. van Dijk and M. J. Wiggers de Vries: Determination and adjustment of the activity of adsorbents for chromatography and of the eluting power of elution solvents by means of the "shake test" (Analysis of fat soluble vitamins III) (Rec. Trav. chim. Pays-Bas **76**, 747-756, 1957, No. 8).

Adjustment of the activity of adsorbents for chromatographic use (e.g. Al_2O_3 or $CaHPO_4$ by the controlled take-up of water) can be done in a reproducible and accurate manner with the aid of the "shake test". It consists in shaking a weighed sample (2 g) of the adsorbent with a measured volume (10 ml) of the elution solvent in which the substance to be eluted (e.g. 1000 I.U. of vitamin A) has been dissolved. The activity is suitable if about 50% is adsorbed. The following operations can be performed by means of the shake test: 1) determination of the activity of adsorbents; 2) adjustment of the activity of an adsorbent; 3) replacement of an adsorbent by another of the same activity; 4) finding the correct composition of the elution solvent; 5) replacement of one solvent by another of equal eluting power. The shake test has been developed for a 10 cm column containing 10 g of Al_2O_3; 40% adsorption is satisfactory for rapid elution. If slower elution is wanted, or if thinner columns (containing less adsorbent) are employed, the percentage adsorption must be larger than 40%, up to 60%. The shake test is a purely practical test; no theoretical significance can be attached to it.

2534: A. C. van Dorsten and J. H. Spaa: A high-output D-D neutron generator for biological research (Nucl. Instr. **1**, 259-267, 1957, No. 5).

A description is given of an apparatus capable of producing a fast neutron flux exceeding 10^{10} neutrons per second from a D-D reaction. The set consists of a pressurized cascade generator and an accelerator tube with a rotary heavy-ice target. The rectifiers used are of the selenium type.

2535: F. W. Klaarenbeek and M. H. de Lange: Enkele aspecten van de warmtetechniek van glassmeltovens (Ingenieur **69**, W137-W140, 27 Sept. 1957). (Some aspects of heating techniques in glass furnaces; in Dutch.)

A brief description is given of the melting process of glass and of the furnaces mostly used. An attempt is made to formulate the requirements of these furnaces. Some experiences from industrial practice are compared with the results of flame research at IJmuiden (Netherlands).

2536: J. Volger: Dielectric loss in insulating solids caused by impurities and colour centres (Disc. Faraday Soc. No. 23, 63-71, 1957).

Experiments at low temperatures on solids with various lattice defects have revealed the existence of dielectric relaxation phenomena due to these defects. The relaxation times are governed by activation energies far smaller than those normally found with diffusion or migration of ions. Typical measurements are given and discussed qualitatively in relation to models of some lattice imperfections including colour centres.

2537: K. Compaan and Y. Haven: Some fundamental aspects of the mechanism of diffusion in crystals (Disc. Faraday Soc. No. 23, 105-112, 1957).

Diffusion data, if available in the form $D = D_0 \exp(-E/kT)$, yield two parameters, whereas for a molecular description more quantities are needed. Some difficulties encountered with this problem are discussed. This problem has kinetic as well as equilibrium aspects. The equilibrium aspect has been successfully attacked by the theory of lattice defects: it is possible to specify the atoms that are mobile as well as the frequency with which these mobile atoms jump. Recently, a novel kinetic aspect of the mechanism has become of interest, viz., the problem of correlation between the directions of consecutive jumps of an atom. These correlations effectively alter the self-diffusion coefficient in certain mechanisms, but not the diffusion coefficient for drift or the ionic conductivity. The latter aspect has recently been developed to a promising method of disentangling diffusion mechanisms, especially in ionic crystals.

2538: E. J. W. Verwey: Onderzoekingen over oxydische ijzerverbindingen (Versl. gew. Verg. Afd. Natuurk. Kon. Ned. Akad. Wet. **66**, 106-110, 1957, No. 7). (Investigations on oxidic iron compounds; in Dutch.)

Short survey article on investigations on hexagonal ferrites carried out in recent years at the Philips Research Laboratories. These ferrites, apart from various small metal ions, always contain at least one type of metal ion of larger radius, e.g. Ba^{2+}. The crystal structures of a number of compounds of the ternary system BaO-Fe_2O_3-MeO are discussed (Me is a metal with small ionic radius). All these compounds have structures closely related to close-packed structures of the large ions (O^{2-} and Ba^{2+}). The unravelling of these structures has been accomplished by X-ray crystallographic methods. The magnetic properties of these compounds are the most important from the point of view of practical applications. (See Philips tech. Rev. **13**, 181-193, 1951/52, and **18**, 145-154, 1956/57.)

2539: L. A. Æ. Sluyterman: The amperometric titration of sulfhydryl groups with silver nitrate (Biochim. biophys. Acta **25**, 402-404, 1957, No. 2).

Three out of five sulfhydryl-containing compounds, subjected to amperometric titration with silver nitrate, appear to combine with more Ag than corresponds to their sulfhydryl content.

2540: K. Teer: Colour television transmission — practical aspects of the two-sub-carrier system (Electron. Radio Engr. **34**, 280-286 and 326-332, 1957, Nos. 8 and 9).

In recent years a colour-television transmission system using two sub-carriers for the transmission of the chrominance information has been developed. Practical results were demonstrated to Study Group XI of the C.C.I.R. in 1955 and 1956. The principles and evolution of the system have been described and discussed in previous articles. In this article the technical aspects are considered in more detail and data are given about modifications and improvements which have since been introduced.

2541: J. J. Balder: Erwünschte Leuchtdichten in Büroräumen (Lichttechnik **9**, 455-461, 1957, No. 9). (Preferred values of luminances in office rooms; in German.)

A series of tests has established what luminance values the working surface, walls and ceiling should have in office rooms in order to make the surroundings as agreeable as possible to work in. The illumination system used during the tests was ideal in the sense that light falling on the working surface comes from the right directions, and the field of vision contains no disagreeably high luminances of lamps or reflections.

2542: L. F. Defize: Fysische verschijnselen in de lasboog (De metallurgie van het lassen van staal, Lassymposium 1957, published by Ned. Ver. voor Lastechniek, The Hague, pp. 5-11). (Physical phenomena in the welding arc; in Dutch.)

The phenomena involved in gas discharges at atmospheric pressure are of a complex nature. Although the application of arc welding has grown enormously in the last twenty years, only a very limited number of papers dealing with the theory of the arc have appeared. In the arc there is the extra complication that the arc is continuously

interrupted by the droplet transfer. Most investigations on the arc discharge have therefore been made using non-consumable electrodes (carbon arc welding and gas-shielded tungsten arc welding). This paper discusses the cathodic and anodic mechanisms, the questions of the extremely high temperature of the arc and the heating effects at the electrodes. In addition to the D.C. arc, welding with A.C. is also discussed and finally the mechanism of droplet transfer is briefly considered.

2543: J. D. Fast: De rol van gassen bij het booglassen van staal (De metallurgie van het lassen van staal, Lassymposium 1957, Ned. Ver. voor Lastechniek, The Hague, pp. 12-17). (The part played by gases in the arc welding of steel; in Dutch.)

In arc welding of steel with coated electrodes, oxygen, nitrogen and hydrogen are taken up by the carbon-containing weld metal, the amounts taken up being mainly determined by the composition of the coating. In general no equilibria are established and the amounts of the gases taken up cannot therefore be calculated, but nevertheless the laws of chemical equilibrium do enable us to draw a few important conclusions of a qualitative nature. Two of the most important conclusions are: 1) the more stable the oxides of the coating, the less oxygen will be absorbed by the metal; 2) if the water content of the coating remains constant, the amount of hydrogen taken up by the metal will be greater the smaller the amount of oxygen taken up. When the metal solidifies, part of the C, O, N and H present is given off in the form of CO, CO_2, H_2O, H_2 and N_2. Under adverse conditions the evolution of these gases may lead to porosity of the weld. The role played by sulphur in this connection is discussed. The deleterious effects of oxygen, nitrogen and hydrogen left in the metal after solidification, especially aging effects, are also discussed. On the basis of dislocation theory, tentative conclusions can be arrived at regarding the influence of interstitial elements on the brittle fracture of steel and on the different sensitivities of ferritic and austenitic steels to these impurities.

H 1: F. Karstensen: Preferential diffusion of Sb along small-angle boundaries in Ge and the dependence of this effect on the direction of the dislocation lines in the boundary (J. Electronics and Control **3**, 305-307, 1957, No. 3).

Note reporting experiments which show that the rate of diffusion of antimony along the dislocation lines forming a small-angle boundary in germanium exceeds that of self-diffusion in germanium. No such effect is observed in the crystal boundary perpendicular to the dislocation lines.

NOW AVAILABLE

J. D. Fast, H. G. van Bueren and J. Philibert (editors): La diffusion dans les métaux (Philips Technical Library, 1957; pp. 115, 84 figures).

This book (published only in French) forms a record of the papers presented at a colloquium held at Eindhoven in September 1956 on the subject of diffusion in metals. The first paper gives an introductory survey and, of the following papers, two are concerned with the effect of structural defects on the diffusion, four on the Kirkendall effect, two on the diffusion of interstitial atoms and one on the effect of elastic stress on diffusion. The English titles of the papers are as follows: Introduction to the study of diffusion, by A. D. le Claire; The diffusion of radio-tracers in solids, by K. Compaan and Y. Haven; Intergranular diffusion and its relation to grain boundary structure, by P. Lacombe; Intergranular self-diffusion of α-iron, by C. Leymonie and P. Lacombe; New observations on the Kirkendall effect and on electrolytic transport in solid alloys, by Th. Heumann; An electron-beam micro analyser and its use in the study of intermetallic diffusion, by J. Philibert; Study of the diffusion uranium-zirconium in the γ phase, by Y. Adda and J. Philibert; The Kirkendall effect and diffusion in the system gold-platinum, by A. Bolk and T. J. Tiedema; Diffusion of interstitial atoms, by J. L. Meijering; Study of the non-steady permeation of helium through silicon and germanium by means of a mass spectrometer, by A. van Wieringen; Effect of elastic deformation on the mobility of vacancies in copper, by C. W. Berghout.